The text in bold black font are the reviewers' comments.

The text in black font are the authors' answers to the reviewers' comments.

The text in red font are the specific changes made to the final manuscript as a response to the reviewers' comments.

RC1

General comments:

This paper examines eight global hydrologic models (GHMs) across the Amazon basin for several basic performance metrics. The model configurations allow for somewhat limited comparisons of coarse granularity methodological choices (e.g. routing model, input forcing data) across the performance metrics for a subset of the GHMs. The submission is easy to read and logically organized with clearly stated objectives. The overall conclusion that the precipitation dataset may be the most important for essentially uncalibrated GHMs and that calibration of the routing model using daily KGE as the objective function has limited effectiveness, particularly for floods, intuitively make sense and agree with the presented results. While not particularly novel, they are useful conclusions to reiterate to the GHM model development and user community.

We thank Dr. Newman for his useful evaluation of the manuscript and suggestions for improvement. We will address these in the revised manuscript, as according to our responses to each comment below.

Specific comments:

1) This paper suffers from the same issues all macroscale intercomparison studies do. In general the analysis is somewhat superficial and the conclusions regarding which modeling component is best (e.g. routing or hydrologic model) are limited to that very coarse scale. Also, while I do appreciate that the authors describe their model selection efforts, it remains that only a subset of the model decision matrix is populated in an adhoc manner. This limits comparisons and conclusions to specific subsets of models depending on the question asked.

It may be beneficial for the authors to add some statements describing the limitations of these types of studies. For example, question 3.3 examines routing models, but the comparison is for one hydrologic model and one precipitation dataset only. The conclusions in this section are reasonable for that specific comparison; the results may change given another modeling chain upstream of the routing model. When discussing future work/paths forward, it may be helpful to talk about increasing the granularity at which modeling decisions are tested and filling out the model decision matrix in a more quantitative way so that more generalized conclusions can be made.

Overall, we agree with the limitation of comparing only macroscale features between each GHM (e.g. routing model/precipitation forcing) and the suggestion to explicitly highlight some of these limitations. As Dr. Newman mentions, we do highlight the reasoning behind the model and comparison selections in the manuscript with acknowledgment to alternative methodologies.

We plan to change the sub-heading for Sect. 3.6 to "Limitations and future work" by discussing the limitations of using a macroscale intercomparison approach. We will add to the discussion the possibility to expand the study by increasing the granularity at which modelling decisions are tested; thereby allowing more generalised conclusions to be made.

Sect. 3.7 has now been changed to "Limitations and future work" and includes the limitations of macroscale intercomparison modelling studies. See P19 L29-32 and P20 L1-8.

2) There are references relevant to the routing model calibration discussion the authors should consider. Their conclusion that performance is improved for metrics more closely related to the objective function is correct, however the statements on page 17, lines 13-15, and again on page 18, lines 4-5 need further elaboration. Gupta et al. (2009) and Mizukami et al. (2019) discuss in detail how squared error metrics relate to high flow performance. Mizukami et al. (2019) also show how an application specific metric, annual peak flow bias (APFB) can improve model performance for that specific metric, but at the expense of decreased performance in related metrics. This is directly relevant to the final sentence of the conclusions section, and it would be good to note that some application specific metrics could degrade model performance for other parts of the hydrograph, so thoughtful consideration to the full use of the modeling system should be given when performing parameter optimization.

We thank Dr. Newman for this very useful suggestion. We agree that the original conclusion would benefit from further elaboration and evidence from previous works.

We will incorporate both the suggested references to support our discussions and conclusions. Specifically:

i)   By commenting on the suitability of square error related metrics for model calibration when the application requires robust performance for high flows (in Sect. 3.6)
ii) By providing the example of increased model performance when using application specific metrics (i.e. Annual Peak Flow Bias), as in Mizukami et al. (in review)
iii) By discussing the need to carefully consider the metric used in calibration, with the possibility of a loss in skill for other related metrics upon evaluation when using application specific metrics (Sect 3.6 and Sect. 4)

Comments in relation to square error related metrics have been included to P18 L8-14. Comments in relation to increased model performance when using application specific metrics have been included to P19 L13-18. Comments discussing the potential of a loss of skill have been included on P20 L29-31 and P21 L1-2. Both of the suggested references have been included.

RC2

Overall comment:

This manuscript assesses the performance of eight different global hydrological models for 75 gauging stations across the Amazon basin. It assesses the ability of the model to reproduce daily and peak river flows and finds interesting regional differences in model performance. It concludes that the rainfall product is the dominant control on model performance. Overall, I enjoyed reading the paper. It is well-written and logically structured, with excellently formatted plots. While the analysis and results (as Reviewer 1 also pointed out) are not ground-breaking, the work represents a potentially useful contribution to the application of GHMs and their use for flood risk assessment and forecasting. For the results to have wider applicability, I think the authors should consider adding some additional analyses to strengthen their conclusions. Many reasons for good/bad model performance are postulated in the results section but the analysis isn't in-depth enough to draw strong conclusions (other than rainfall is a dominant control on model

performance). The wider applicability of the results also needs to be better highlighted in the conclusions.

We thank Dr. Coxon for her useful evaluation of the manuscript and kind comments. The specific comments are particularly helpful and will improve the overall quality of the paper. We will address these in the revised manuscript, as according to our responses to each comment below.

Specific comments:

1) The authors conclude that rainfall is (unsurprisingly) the dominant control on model performance. If the choice of precipitation dataset is the most influential on model performance then I would have expected a little more analysis on the precipitation datasets themselves. I appreciate that more involved analysis looking at the seasonal characteristics of the rainfall patterns is probably beyond this paper, however a figure of mean annual rainfall across all the catchments for each rainfall product would be useful for the reader to better understand how and why model performance may vary between the different models across the Amazon basin.

We agree with Dr. Coxon that further evaluation of the rainfall products would be beneficial in further understanding differences in model performance given the importance of rainfall in the ability to accurately represent peak flows.

We propose to incorporate a Figure showing mean annual rainfall across the basin for each rainfall product in Sect. 3.4.

A Figure showing mean daily rainfall for ERA-Interim, ERA-5 and the ECMWF 20- year reforecasts for the validation period (1997-2015) has now been included (Fig. 8). The Figure is referred to in Sect. 3.4, P15 L22-26, amongst other locations throughout the results and discussions.

2) P10 L23 "An average of 81% of stations are considered skillful (i.e. > 0) for the KGE metric". I would not consider a KGE score just greater than 0 as 'skillful'. You should be more specific here about what a KGE score greater than zero represents if you are using it as a benchmark to define whether a model is skilful or not. Unlike NSE, a KGE score of zero does not represent the mean streamflow response.

We thank Dr. Coxon for this useful comment. We propose to remove such statements from the manuscript. A similar study (Thiemig et al., 2018) provides a breakdown of KGE (though for the modified version of KGE) results into "good" (KGE > 0.75), "intermediate" (0.75 > KGE > 0.5, "poor" (0.5 > KGE > 0) and "very poor (KGE < 0)" categories. We now plan to use these categories as the benchmark but generally refer to KGE performance as being better as values approach one.

Thiemig, V., Bisselink, B., Pappenberger, F., & Thielen, J.: A pan-African medium-range ensemble flood forecast system. Hydrol. Earth Syst. Sci, 19, 3365-3385, https://doi.org/10.5194/hess-19-1-2015, 2015.

Such statements have now been removed. In Sect. 2.3.2 we have included a breakdown of KGE scores into benchmark categories, as in Thiemig et al. (2015). See P10 L6-15.

3) P10 L27 (and elsewhere). Your 'average' station scores could be skewed here by particularly low values of KGE – it may be better to report the median station scores here instead.

We again thank Dr. Coxon for raising this relevant point. We will change all reported mean values to median values.

All reported mean scores have now been replaced by median values throughout the manuscript, including those in Table 2.

4) Section 3.1. I liked your analysis of the relationship between model performance and dams and Figure 1b. However, as you note, this doesn't fully explain regional differences in model performance. Are there any other catchment characteristics that may also explain good/poor model performance? I would calculate and add some additional catchment characteristics such as mean rainfall, mean pet, elevation, geology (as you also focus on groundwater parameterisation) to Figure 1 to better analyse these regional differences in model performance and strengthen the conclusions of the paper.

As Dr. Coxon mentions, damming in the Amazon is one of many catchment characteristics that could influence model performance. We agree that by including additional characteristics such as rainfall and geology, stronger conclusions can be drawn on regional model performance. For example, Paiva et al. (2013) indicate that poorer model performance in western tributaries could be associated with the poor representation of mountainous rainfall when using satellite-based products such as TRMM. While in Sect 3.1 we hypothesis that the underestimation of flows in stations located in the south eastern Amazon could be due to a poor representation of the South Atlantic Convergence Zone (SACZ). By adding rainfall maps to Fig. 1 or elsewhere (e.g. Sect. 3.4) these statements will be strengthened.

de Paiva, R. C. D., Buarque, D. C., Collischonn, W., Bonnet, M. P., Frappart, F., Calmant, S., & Mendes, C. A. B.: Large-scale hydrologic and hydrodynamic modeling of the Amazon River basin, Water Resour. Res., *49*, 1226-1243, https://doi.org/10.1002/wrcr.20067,2013, 2013.

Maps showing the geology and elevation for the Amazon basin have now been included in Fig. 1. Reference to these Figures can be found in Sect. 3.1, P12 L30-32 and P13 L1-5.

5) Section 3.1. In addition to comment 4 – do any of the GHMs include schemes to represent dams/reservoirs? Do you see any differences in model performance for models that do include these human influences over models that do not?

This is an interesting point. Model runs which incorporate the Lisflood routing model (i.e. those similar to the current GloFAS set-up) represent a total of 464 lakes and 667 reservoirs obtained from global databases. Very few reservoirs however are represented in the Amazon basin for Lisflood with the majority of lakes positioned along the main Amazon River. The locations and importance of these to the modelling system has been analysed by Zajac et al. (2017) for the entire globe with the effects of reservoirs on extreme high flows deemed substantial and widespread in the global domain. All other simulations do not account for dams/reservoirs and thus comparison between these runs could strengthen our understanding of why some models perform particularly well or poor at the few stations affected.

We will add information regarding the representation of lakes and reservoirs within Lisflood in Sect. 2.2.3. In addition, we will investigate the potential benefits or losses in skill by comparing model performance at stations located near to any reservoirs between Lisflood and non-Lisflood

simulations. Although the number of stations effected will be limited it could still provide useful information.

Zajac, Z., Revilla-Romero, B., Salamon, P., Burek, P., Hirpa, F. A., & Beck, H.: The impact of lake and reservoir parameterization on global streamflow simulation, J. Hydrol., 548, 552-568, https://doi.org/10.1016/j.jhydrol.2017.03.022, 2017.

Details describing the representation of lakes and reservoirs in Lisflood has been included in Sect. 2.2.3, P8 L23-28. A paragraph has been included in Sect. 3.3, P15 L3-10 discussing the potential benefits or losses in skill.

6) Conclusions L28-29. You state that "The implications of these results suggest that the choice of precipitation dataset is the most influential component of the GHM set-up in terms of our ability to recreate annual maximum river flows in the Amazon basin". Can you say anything more about what type or spatial resolution of precipitation dataset should be used to better reproduce annual maximum flows? This would help to guide future studies on modelling peak flows in the Amazon basin.

We agree that statements regarding the type of spatial resolution required would be beneficial for future studies modelling peak flows in the Amazon basin. However, it would be difficult to make direct statements (e.g. provide a specific spatial resolution) based on our results alone owing to the conclusions being specific to the few directly comparable datasets (i.e. ERA-I Land, ERA-5 and ECMWF 20- year reforecasts forced within the calibrated Lisflood model) used. We can, however, as mentioned in Sect. 3.4, elude to specific cases which may benefit from using certain datasets. For example, those wishing to model peak flows in the Peruvian Amazon may benefit from a dataset where the upper atmosphere is resolved at a higher resolution owing to those particular rivers originating from mountainous regions where rainfall can often be poorly represented (e.g. Paiva et al., 2013).

We plan to expand on our discussions, particularly in Sect. 3.4, to include further findings from studies such as Beck et al. (2017) whereby 22 precipitation products are evaluated across the globe. This could help explain further our results and allows us to strengthen our conclusions on why particular datasets lead to particularly good or bad performance in certain regions.

Beck, H. E., Vergopolan, N., Pan, M., Levizzani, V., van Dijk, A. I., Weedon, G. P., & Wood, E. F.: Global-scale evaluation of 22 precipitation datasets using gauge observations and hydrological modeling. Hydrol. Earth Syst. Sci, 21, 6201-6217, https://doi.org/10.5194/hess-21-6201-2017, 2017.

Further statements regarding the type or spatial resolution of precipitation dataset has been included in Sect. 3.4, P17 L6-10 and in Sect. 4, P20 L18-24.

Assessing the performance of global hydrological models for capturing peak river flows in the Amazon Basin

Jamie Towner[1], Hannah L. Cloke[1,2,4,5], Ervin Zsoter[3,1], Zachary Flamig[6], Jannis M. Hoch[7,8], Juan Bazo[10,11], Erin Coughlan de Perez[9,10], Elisabeth M. Stephens[1]

[1]Department of Geography & Environmental Science, University of Reading, Reading, RG6 6AB, UK
[2]Department of Meteorology, University of Reading, Reading, RG6 6BB, UK
[3]European Centre for Medium-Range Weather Forecasts, Shinfield Park, Reading, RG6 9AX, UK
[4]Department of Earth Sciences, Uppsala University, Uppsala, 752 36, Sweden
[5]Centre of Natural Hazards and Disaster Science, CNDS, Uppsala, 752 36, Sweden
[6]University of Chicago Center for Data Intensive Science, Chicago, USA
[7]Department of Physical Geography, Utrecht University, P.O. Box 80115, 3508 TC Utrecht, the Netherlands
[8]Deltares, P.O. Box 177, 2600 MH Delft, the Netherlands
[9]International Research Institute for Climate and Society, Columbia University, Palisades, NY 10964, USA
[10]Red Cross Red Crescent Climate Centre, The Hague, 2521 CV, the Netherlands
[11] Universidad Tecnológica del Perú (UTP), Lima, Perú

Correspondence to: Jamie Towner (j.towner@pgr.reading.ac.uk)

Abstract. Extreme flooding impacts millions of people that live within the Amazon floodplain. Global Hydrological Models (GHMs) are frequently used to assess and inform the management of flood risk, but knowledge on the skill of available models is required to inform their use and development. This paper presents an intercomparison of eight different GHMs freely available from collaborators of the Global Flood Partnership (GFP) for simulating floods in the Amazon basin. To gain insight into the strengths and shortcomings of each model, we assess their ability to reproduce daily and annual peak river flows against gauged observations at 75 hydrological stations over a 19-year period (1997-2015). As well as highlighting regional variability in the accuracy of simulated streamflow these results indicate that a) the meteorological input is the dominant control on the accuracy of both daily and annual maximum river flows, and b) groundwater and routing calibration of Lisflood based on daily river flows has no impact on the ability to simulate flood peaks for the chosen river basin. These findings have important relevance for applications of large-scale hydrological models, including analysis of the impact of climate variability, assessment of the influence of long-term changes such as land-use and anthropogenic climate change, the assessment of flood likelihood, and for flood forecasting systems.

1 Introduction

Flooding is notably the most common and damaging natural hazard affecting millions of people worldwide every year, producing economic losses exceeding billions of dollars (Hirabayashi et al., 2012). Flood risk associated to a particular location can be highly variable depending on levels of exposure, resilience and preparedness (Alfieri et al., 2018) in addition to the increased uncertainty surrounding trends of hydrological extremes in a warming climate (Arnell and Gosling, 2016).

1

For the Amazon basin, flood risk is considered to have increased, with a greater frequency of extreme flood events (e.g. in 2009, 2012 and 2014; Marengo and Espinoza, ~~2015~~2016) coinciding with a hypothesised intensification of the hydrological cycle since the 1980's (Gloor et al., 2013). Floods in Amazonian communities are known to have large socioeconomic consequences impacting eco-systems, health, transport links and are particularly damaging to agricultural and fishery

5 practices (Schöngart and Junk 2007; Marengo et al., 2012; Marengo et al., ~~2014~~2013; Correa et al., 2017). Single flood events (e.g. 2012 in the Amazonian city of Iquitos, Peru) have impacted the lives of over 73,000 people (IFRC, 2013) with average annual damages estimated at 1.4 billion USD over a four-year period (2008-2011) in the Brazilian Rio Branco river basin alone (Mundial Grupo Banco, 2014).

1.1 Global hydrological models and applications

10 In its simplest form, a hydrological model can be considered a representation of a real-world hydrological system used to better understand various water and environmental processes, predict system behaviour and provide consistent impact assessment (Devia et al., 2015). They work by simulating the hydrological response to meteorological variations incorporating run-off generation and river routing processes (Sutanudjaja et al., 2018). As such, Global Hydrological Models (GHMs) have been used in a wide range of applications including short to extended-range flood forecasting (Alfieri et al.,

15 2013; Emerton et al., 2018), climate assessment (Hattermann et al., 2017), hazard and risk-mapping (Ward et al., 2016), drought prediction (van Huijevoort et al., 2014) and water resource assessment (e.g. water availability models; Meigh et al., 1999; Sood & Smakhtin, 2015).

Depending on the application and the needs of decision makers, different properties of the hydrograph simulated by hydrological models are important. For example, an accurate representation of peak river flows and their likelihood is key

20 for decision-makers who wish to understand the area at risk of flooding. In contrast, estimates of daily streamflow may be more beneficial for the assessment of water resources such as irrigation requirements.

1.2 GHM development

The availability of GHMs has grown in recent years thanks to increased efforts in addressing water related issues in developing countries (De Groeve et al., 2015; Ward et al., 2015; Trigg et al., 2016), the development of flood forecasting

25 systems (Aliferi et al., 2013; Werner et al., 2013; Emerton et al., 2018), improvements within precipitation datasets (Mittermaier et al., 2013; Novak et al., 2014; Forbes et al., 2015), the emergence of new global satellite and remote sensing datasets and advancements in numerical modelling techniques (Yamazaki et al., 2014a; Sampson et al., 2015; Andreadis et al., 2017; Balsamo et al., 2018). For an overview of available GHMs see Bierkens et al. (2015) who have provided the details of 22 large-scale hydrological models with those used for operational flood forecasting being summarised in Emerton

30 et al. (2016).

1.3 Land surface models vs hydrological models

GHMs have differing spatial and temporal resolutions, parameter estimation approaches, number of parameters, calibration methods, input-output variables and overall ~~structure~~structures (Sood and Smakhtin, 2015). Their set-ups can generally be divided into two categories: Land Surface Models (LSMs) and hydrological models (Gudmundsson et al., 2012). The

5   majority of LSMs and hydrological models share the same conceptualisation of the water balance (Haddeland et al., 2011) but differ in their objective. LSMs evolve from coupled land/atmosphere models with the purpose of solving the surface energy balance equations to provide the necessary lower boundary conditions to the atmosphere (Wood et al., 2011). In contrast, hydrological models tend to focus less on the partitioning of radiation and more on hydrological resources and understanding the lateral movement and transport of water along the land surface.

10 In terms of differences in model performance, the Gudmundsson et al. (2012) intercomparison study of six LSMs and five GHMs (i.e. hydrological models) concluded that the main differences were due to the snow scheme implemented with snow water equivalent values and mean runoff fractions lower in LSMs. No significant differences between LSMs and hydrological models were found for runoff and evapotranspiration globally but rather the differences between the models themselves created large sources of uncertainty, highlighting the importance of analysing a range of different GHMs rather

15 than a group consisting of a specific model type. For the purposes of this study, we categorise both LSM and hydrological models as GHMs.

1.4 Motivation

For GHMs to be considered effective, end users need to know their accuracy and reliability (Ward et al., 2015). Thus, the evaluation of these models against observed data is an important procedure in efforts to reduce flood risk. Currently, no

20 intercomparison analysis of GHMs has been conducted specifically for the Amazon basin with previous studies focusing solely on the performance of individual models for the Amazon (e.g. Yamazaki et al., 2012; Paiva et al., 2013; Hoch et al., 2017a; Hoch et al., 2017b) or as part of a global study (e.g. Gudmundsson et al., 2012; Alfieri et al., 2013; Hirpa et al., 2018~~)~~), which lack an in-depth focus on skill within the Amazon basin.

Finally, many of the GHMs (or their components) analysed in this study are used for specific applications. For instance,

25 water resources management (PCRaster Global Water Balance; PCR-GLOBWB), flash flood forecasting (Ensemble Framework for Flash Flood Forecasting; EF5) and extended-range flood forecasting (Global Flood Awareness System; GloFAS). Investigating the performance of hydrological simulations therefore can provide valuable information to researchers and model developers with which to better understand some of the strengths and weaknesses which exists within the model set-ups and help to distinguish how different parts of the hydrological chain can cause ~~particular~~particularly

30 'good' or 'bad' model performance; thus, having implications for their different applications.

1.5 Objectives

In this study, the main objective is to assess the ability of different GHMs freely available from collaborators within the Global Flood Partnership, (GFP), identifying which approaches are most suitable in different areas of the Amazon basin for simulating flood peaks. To pursue this objective, the analysis is designed to answer the following research questions:

5
1. How well do GHMs represent the annual hydrological regime in terms of the Kling-Gupta-Efficiency (KGE) and its individual components?
2. Which model set-up best represents annual maximum river flows?
3. Which hydrological routing model allows the best representation of daily and peak river flows?
4. Which precipitation dataset allows the best representation of daily and peak river flows?
10
5. How do results differ when using a LSM as opposed to a hydrological model?
6. By how much does calibration of groundwater and routing model parameters improve performance?

2 Data and methodology

The experimental design involves comparing the output of daily and annual maximum discharge estimates produced by different GHMs forced using atmospheric reanalysis or satellite precipitation datasets against observations of streamflow.

15 The common validation period is 1997-2015 with results also analysed for the shorter period of 2004-2015 to account for the shorter record length of one simulation.

2.1 Observations

Observed daily discharge data is used to evaluate each of the model runs. The network of hydrometric gauges is controlled and maintained by the national institutions responsible for hydrological monitoring in countries situated within the Amazon

20 basin. These include: Agência Nacional de Águas (Water National Office – ANA, Brazil), Servicio Nacional de Meteorología e Hidrología (National Meteorology and Hydrology Service – SENAMHI, Peru and Bolivia), Instituto Nacional Meteorologia e Hidrologia (Institute to Meteorology and Hydrology, INAMHI, Ecuador) and the Instituto de Hidrología, Meteorología y Estudios Ambientales (Institute of Hydrology, Meteorology and Environmental Studies - IDEAM, Colombia).

25 Daily water level values are collected by the respective institution and are sourced through the ORE-HYBAM observational service (see http://www.ore-hybam.org/) or directly from the national services. A time series of daily river flow for each station is obtained using stage and rating curve measurements which were determined using an acoustic Doppler current profiler (ADCP) conducted by the ORE-HYBAM observatory and SENAMHI (Espinoza et al., 2014). In total 75 hydrological stations throughout the Amazon basin are selected with an average record length of 17 years within the main

30 validation period (1997-2015). The locations of stations and their characteristics are displayed in Fig. 1a and Table S1

respectively. Stations selected have a minimum of five consecutive years' worth of data during the main validation period. The threshold was set to five to prevent the elimination of stations in data scarce areas such as Peru, Bolivia and Colombia.

2.2 Routing models and meteorological datasets

Eight GHMs composed of different meteorological datasets, hydrological/LSMs and river routing models, are used to each
5 simulate river discharge across the Amazon basin. Four meteorological products (ERA-Interim Land re-analysis, ERA-5 re-analysis, ECMWF 20-year control reforecasts (hereafter used as reforecasts) and the real-time TRMM TMPA 3B42 v.7), three hydrological/LSM (PCR-GLOBWB, the Hydrology-Tiled ECMWF Scheme for Surface Exchanges over Land; H-TESSEL, EF5) and three river routing models (Catchment-based Macro-scale Floodplain model; CaMa-Flood, Lisflood and the Coupled Routing and Excess Storage; CREST) are employed. While the focus of this study is on GHMs made available
10 by the GFP community, other models are available within the Amazon basin. Some examples include: MGB-IPH (Paiva et al., 2013), LPJmL (Lund–Potsdam–Jena managed Land; Bondeau et al., 2007), WaterGAP (water - global analysis and prognosis; Döll et al., 2003) and MAC-PDM.09 (the Macro-scale-Probability-Distributed Moisture model.09; Gosling & Arnell, 2011).

As a result of using freely available datasets from collaborators within the GFP, simulations are composed of a combination
15 of routing models and meteorological datasets and do not all use the same precipitation input or hydrological set-up. However, the available combinations allow enough insight into the model components to draw conclusions for the objectives stated. For example, to analyse the performance of precipitation inputs, ERA-Interim Land, ERA-5 and the reforecasts are forced through the calibrated version of Lisflood, whereby the routing and LSM remain consistent. To evaluate the differences between using the Lisflood and CaMa-Flood routing models, two simulations which use ERA-Interim Land
20 precipitation and the LSM H-TESSEL are compared. To identify the differences between employing a hydrological (PCR-GLOBWB) or LSM (H-TESSEL), two set-ups which use the ERA-Interim Land precipitation reanalysis and the CaMa-Flood river routing model are directly compared. Finally, to see how much benefit model calibration within Lisflood provides, ERA-Interim Land and ERA-5 are forced through the calibrated and un-calibrated Lisflood model versions. The CREST EF5 run is the sole simulation to have a unique hydrological model and meteorological input and although it is more
25 challenging to analyse the performance of specific components of the model set-up against other simulations, it was included in the analysis for completeness.

An alternative approach would be to implement a full intercomparison experiment and run a new set of simulations which included all combinations of precipitation input, GHM and routing scheme. However, this is a very large undertaking and the time and computational expense to achieve this is prohibitive. Instead, by using freely available datasets with different
30 hydrological set-ups, our method allows a first analysis providing enough evidence of dataset reliability and accuracy in order to determine the utility of the differing approaches for climate studies and to forecast applications. Moreover, by using iterative runs of similar model set-ups (i.e. changing a specific part of the hydrological model chain) it allows us to make

conclusive statements regarding the differences in skill. Finally, a short description of each model and atmospheric product is outlined below with a summary of each simulation provided in Table 1.

2.2.1 Precipitation datasets

ERA-Interim Land is a global reanalysis of land surface parameters produced by the European Centre for Medium-range
5   Weather Forecasts (ECMWF) with a T255 spectral resolution (~80 km or ~0.75^0): Balsamo et al., 2015). ERA-Interim Land was produced using the latest version of the land surface H-TESSEL model using atmospheric forcing from ERA-Interim (Dee et al., 2011), with precipitation adjustments based on the Global Precipitation Climate Project (GPCP) v2.1. Precipitation improvements were achieved by Balsamo et al. (2010) using a scale-selective rescaling procedure in which ERA-Interim 3-hourly precipitation were corrected to match the monthly accumulation provided by the GPCP at grid point
10   scale (Huffman et al., 2009). All simulations which use ERA-Interim Land are run offline to force the associated rainfall-runoff models (see Table 1). For a detailed description of the ERA-Interim Land and ERA-Interim datasets see Balsamo et al. (2015) and Dee et al. (2011) respectively. Dataset available at: <http://apps.ecmwf.int/datasets/data/interim-full-daily/levtype=sfc/>.

ERA-5 is the latest reanalysis product of the ECMWF producing consistent estimates of atmospheric, land and ocean
15   variables at a horizontal resolution of ~31 km, while the vertical atmosphere is discretised into 137 levels to 0.01 hPa (ECMWF, 2018). ERA-5 is based on the Integrated Forecasting System (IFS) Cycle 41r2 which was used operationally at the ECMWF in 2016. Early analysis has shown that ERA-5 has an improved representation of precipitation (particularly over land in the deep tropics), evaporation and soil moisture compared to its predecessor ERA-Interim Land (ECMWF, 2017). ERA-5 is currently being produced in three "streams" and will eventually cover the period 1950 to near real-time (~3
20   days) with completion due in 2019 (Emerton et al., 2018). Dataset available at: <https://software.ecmwf.int/wiki/display/CKB/How+to+download+ERA5+data+via+the+ECMWF+Web+API>.

ECMWF reforecasts are a collection of historical forecasts from start dates at the same day of the year going back for a specific number of years to provide a consistent model climatology from which to compare forecasts (ECMWF, 2016). In this study we use the control member of the reforecasts which are created based on a retrospective run of the most recent
25   version of the ECMWF's IFS to provide surface and subsurface runoff as input to the Lisflood routing model at a resolution of 0.1^0. The reforecast run is computed using a lighter configuration (11 ensemble members, run twice a week on Mondays and Thursdays) to reduce computational time. The purpose of running the ECMWF forecasts through the Lisflood routing model is to generate a long term (20-year) dataset which is consistent with operational GloFAS forecasts enabling the suitability of the dataset for use in the calibration of the Lisflood model parameters (Hirpa et al., 2018). This data covers the
30   period June 1995 to June 2015 and due to frequent model updates of the IFS, is based on multiple model cycles: Cycle 41r1 (July through March) and Cycle 41r2 (March through June). The control reforecasts from Mondays and Thursdays are used subsequently to fill the whole weeks by taking the first 3- and 4-day forecast periods respectively throughout the 20 years.

TRMM TMPA 3B42 RT v7 is a global merged multi-satellite precipitation product generated at the National Aeronautics and Space Administration (NASA). TMPA is computed for two products: a near real-time version (TMPA 3B42RT v7) and a post real-time gauged adjusted research version (TMPA 3B42 v7), both of which run at resolution of 3 hourly x 0.25^0 x 0.25^0 (Huffman et al., 2007). The TMPA 3B42 RT gridded dataset used in this study covers the global latitude belt from 60^0

5   N to 60^0 S. For further information see Huffman et al. (2007). Dataset available at: < https://pmm.nasa.gov/data-access/downloads/trmm>.

2.2.2 Hydrological and land surface models

H-TESSEL provides the land surface component of the ECMWF IFS (van den Hurk et al. 2000; van den Hurk and Viterbo 2003; Balsamo et al. 2009). H-TESSEL simulates the land surface response to atmospheric conditions estimating water and

10 energy fluxes (heat, moisture and momentum) on the land surface (Zsoter et al., ~~in review~~2019). H-TESSEL is predominately used within the operational set-up of short to seasonal-range weather forecasts coupled with the atmosphere, but it can also be used in an "offline mode" to calculate the land surface response to atmospheric forcing, whereby input data (e.g. near surface meteorological conditions) is provided on a 3 hourly timestep (Pappenberger et al., 2012). In this study, H-TESSEL receives boundary conditions from the atmospheric input provided by either the ERA-5 reanalysis, ERA-Interim

15 Land reanalysis or the reforecasts providing total runoff for the CaMa-Flood routing model, and the surface and sub-surface water fluxes for Lisflood. Runs forced using the ERA-Interim Land reanalysis are run in the offline mode. For a detailed description of H-TESSEL see Balsamo et al. (2009).

PCR-GLOBWB is a global hydrological and water resource model developed at the Department of Physical Geography, Utrecht University, Netherlands (Sutanudjaja et al., 2018). For each grid cell and time step, PCR-GLOBWB simulates

20 moisture storage in two vertically stacked upper soil layers, as well as the water exchange among the soil, the atmosphere, and the underlying groundwater reservoir. Besides, water demands for irrigation, livestock, industry, and households can be integrated within the model. Run-off is routed along a Local Drainage Direction (LDD) network using the kinematic routing wave equation. PCR-GLOBWB was applied at a resolution of 30 arcmin (~ 55km x 55km at the Equator) with meteorological forcing provided from the ERA-Interim Land reanalysis dataset between 1997 and 2015. For further

25 information on PCR-GLOBWB, see van Beek and Bierkens (2008), van Beek et al. (2011) and Sutanudjaja et al. (2018).

EF5 is an open source software package developed at the University of Oklahoma (OU) that consists of multiple hydrological model cores producing outputs of streamflow, water depth and soil moisture (Clark et al., 2016). Since 2016, EF5 has been used operationally for local forecasts across the U.S. National Weather Service (NWS) for flash flooding purposes (Gourely et al., 2017). EF5 incorporates CREST which is a distributed hydrological model created by OU and

30 NASA (Wang et al., 2011). Within CREST, runoff generation, evapotranspiration, infiltration and surface and subsurface routing are computed at each grid cell within the model domain with surface and subsurface water routed using a kinematic wave assumption. Four excess storage reservoirs characterise the vertical profile within a cell representing interception by

the vegetation canopy and subsurface water storage in the three soil layers (Meng et al., 2013). In addition, the representation of sub-grid cell routing and soil moisture variability is made through the use of two linear reservoirs for overland and subsurface runoff individually (Wang et al., 2011). Locations of major streams, flow direction maps and flow accumulation are all derived from the HydroSHEDS dataset (Lenhnar et al., 2008).

5   In this study, an un-calibrated version of EF5 was run using CREST version 2.0 (Xue et al., 2013; Zhang et al., 2015) for 13 years (2003-2015)), with a one-year spin-up at a spatial resolution of 0.05^0 x 0.05^0. Parameters are estimated a priori from soil and geomorphological variables with meteorological forcing provided by the TMPA 3B42 RT product for precipitation and monthly averaged potential evapotranspiration (PET) from the Food and Agriculture Organisation (FAO). For full details on the system set-up see Clark et al. (2016).

10   **2.2.3 Routing models**

Lisflood is a global spatially distributed, grid based hydrological and channel routing model commonly used for the simulation of large-scale river basins (van Der Knijff et al., 2010). It is currently used as an operational rainfall-runoff model within the European Flood Awareness System (EFAS) for streamflow forecasts over Europe (Smith et al., 2016). Unlike EFAS, which uses the full Lisflood set-up, GloFAS and the simulations included in this study use only the routing

15   component of the Lisflood set-up with surface and sub-surface input fluxes (e.g. vertical water, water/snow storage) provided by the H-TESSEL module of the IFS at a resolution of 0.1^0. Surface runoff is routed through Lisflood using a four-point implicit finite-difference solution of the kinematic equations. Sub-surface storage and transport is routed to the nearest downstream channel pixel within one-time step through two linear reservoirs (Alfieri et al., 2013). The water in each channel pixel is finally routed through the river network taken from the HydroSHEDS project (Lenhnar et al., 2008) using the same

20   kinematic wave equations as for the overland flow. Subsurface flow from the upper and lower groundwater zones is routed into the nearest downstream channel as a scaled sum of the total outflow from both the upper and lower groundwater zones. Further details of the Lisflood model is described in van der Knijff et al. (2010).

Lisflood also represents lakes and reservoirs as simulated points on the river network (Zajac et al., 2017). The outflow of lakes and reservoirs are based on: (a) upstream inflow, (b) precipitation over the lake or reservoir, (c) evaporation from the

25   lake or reservoir, (d) the lakes initial level, (e) lake outlet characteristics and (f) reservoir-specific characteristics. For further details on the parameterisation of lakes and reservoirs within Lisflood see Appendix A within Zajac et al. (2017). In the Amazon, represented lakes are predominately located along the main stem with very few reservoirs throughout the basin. For exact lake and reservoir locations within the global Lisflood model see Zajac et al. (2017).

In this study, two set-ups of Lisflood are used (Lisflood_uc and Lisflood_c). Lisflood_c represents the calibrated set-up of

30   the Lisflood routing and groundwater parameters (see Hirpa et al., 2018)-)., while Lisflood_uc representing the uncalibrated model run. Parameters were calibrated with the reforecasts initialised with the ERA-Interim land reanalysis from 1995-2015

as forcing, against observed discharge data at 1278 gauging stations worldwide. All but one station (*40*, see Fig. 1a & Table S1) used in this study were included within the calibration. An evolutionary optimization algorithm was used to perform the calibration with the Kling-Gupta Efficiency (KGE) as the objective function. The calibration was carried out for parameters controlling the time constants in the upper and lower zones, percolation rate, groundwater loss, channel Manning's

5   coefficient, the lake outflow width, the balance between normal and flood storage of a reservoir and the multiplier used to adjust the magnitude of the normal outflow from a reservoir. The results were validated by Hirpa et al. (2018) using the Kling Gupta Efficiency (KGE; Gupta et al., 2009) over the period 1995-2015. In calibration (validation) KGE skill scores were greater than 0.08 compared to the default Lisflood simulation for 67% (60%) of stations globally. For a detailed description of the calibration of the Lisflood parameters and the range of values used for each parameter see Hirpa et al.

10   (2018).

CaMa-Flood is a global distributed river routing model which is forced by runoff input from a LSM or hydrological model to simulate water storage where further hydrological variables (i.e. river flow, water level and inundated area) can be derived along a prescribed river network. Horizontal water transport along the river network is calculated using the local inertia equations (Yamazaki et al., 2011). The backwater effect (i.e. upstream water levels which affect flow velocity downstream,

15   see Meade et al., 1991) is represented by estimating flow velocity based on water slope. (Yamazaki et al., 2011). Moreover, floodplain inundation is represented within CaMa-Flood as a subgrid scale process by discretising the river basin into unit catchments which consist of subgrid river and floodplain topography parameters (Yamazaki et al., 2014b). These parameters describe the relationship between the total water storage in each grid point and water stage and are automatically generated using the Flexible Location of Waterways (FLOW) method with the generation of the river map created by upscaling the

20   HydroSHEDS flow direction map (Lehner et al., 2008). For further information about the CaMa-Flood model see the aforementioned references. In this study, daily river discharge was obtained using CaMa-Flood version 3.6.1 at a spatial resolution of 0.25^0 (~25km grid size) for both runs. The Manning's river and floodplain roughness coefficients were set at 0.03 s $m^{-1/3}$ and 0.10 s $m^{-1/3}$ uniformly for both CaMa-Flood simulations.

2.3 Verification metrics

25   #### 2.3.1 Spearman's ranked correlation

The non-parametric Spearman's rho is used to measure the strength and direction of the monotonic relationship between the ranks of the observed and simulated annual maximum values. The non-parametric Spearman's rho was preferred to the Pearson's statistic as non-parametric measures are less sensitive to outliers in the data and are widely considered a more robust measure of the correlation between observed and predicted values (Legates & McCabe, 1999). Correlation scores for

30   rho range from -1 to 1 with 1 being a perfect correlation. We consider scores which have a value of 0.6 or more to be considered skilful. Similar scores (between 0.5-0.7) are considered to represent a good level of agreement between observed and simulated values in similar studies (see Yamazaki et al., 2012; Alfieri et al., 2013).

2.3.2 KGE

The KGE (Gupta et al., 2009) measures the goodness-of-fit between estimates of simulated discharge and gauged observations and is a modified version of the dimensionless Nash Sutcliffe Efficiency (NSE; Nash and Sutcliffe, 1970). The metric decomposes the NSE into three independent hydrograph components (linear correlation (r), bias ratio (β) and relative

5   variability between the observed and simulated streamflow (α)) by re-weighting the relative importance of each (Revilla-Romero et al., 2015). KGE values range from - ∞ to one with values closer to one indicating better model performance. To provide further context to the computed KGE scores, we use the breakdown of KGE values into four benchmark categories as according to (Kling, 2012). These are classified as follows:

- "Good" (KGE ⩾ 0.75)
10 - "Intermediate" (0.75 > KGE ⩾ 0.5)
- "Poor" (0.5 > KGE > 0)
- "Very poor" (KGE ⩽ 0)

Although originally for the modified version of the KGE, these categories provide an informative benchmark at which to evaluate results. A similar study (Thiemig et al., 2013) assessing the performance of satellite-based precipitation products for

15 hydrological evaluation also adopted the same approach.

When analysing the results, each component of the KGE is also considered independently enabling model errors to be directly related to either the variability (KGE_ α), bias ratio (KGE_ β) or correlation (KGE_r) (; Guse et al., 2017). KGE_α values greater than 1 indicates that variability in the simulated time series is higher than that of the observed. Values less than 1 show the opposite effect. KGE_ β values greater than 1 indicate a positive bias whereby predictions overestimate

20 flows relative to the observed data, while values less than 1 represent an underestimation.

To evaluate the relative improvement of using one model set-up relative to another (e.g. using the calibrated Lisflood routing model as opposed to the uncalibrated model version) metrics are calculated as skill scores:

$$KGE_{SS} = \frac{KGE_a - KGE_{def}}{1 - KGE_{def}}$$ (1)

Where: KGE$_{SS}$ signifies the KGE skill score, KGE$_a$ is the KGE score for the improved run or simulation of interest (e.g.

25 Lisflood_c) and KGE$_{def}$ is the KGE score for the 'default' or comparative run (e.g. Lisflood_uc). Positive KGE$_{ss}$ indicates improved skill whilst a negative score represents a decrease in skill. For each case, KGE scores are calculated against observed river flow data. The correlation skill score is calculated similarly. All metrics are computed in the R environment using the 'verification' (Gilleland, 2015) and 'hydroGOF' (Zambrano-Bigiarini, 2017) R-packages.

3 Results and discussion

To allow for easier interpretation, the results and discussion are separated into six sections which match the research questions presented in Sect. 1.5, in addition to an outline of potential future work. Due to similar results between the two validation periods (1997-2015 and 2004-2015), only results for 1997-2015 are shown. For 2004-2015 results see Figs. S1 &

5   S2. Results and discussions for individual stations are commonly referred to by the station numbers in italics and are presented in Fig. 1a and Table S1.

3.1 How well is the annual hydrological regime represented?

The annual hydrological regime on average is well represented by all models (Fig. 2~~)~~), with the rationale for poorer performance at specific gauges dependent on ~~each model based on~~ either the temporal ~~correction~~correlation, bias ratio or

10   variability ratio components of the KGE (Figs. 3-5). An average of ~~81~~50% of stations ~~are considered skillful (i.e. >~~note scores above 0~~)~~.5 for the KGE metric across all eight simulated runs with a maximum value of 0.92 observed at the Santa Rosa gauging site (*48*, Fig. 1a) for the ERA-5 Lisflood_c simulation (Fig. 2f). The two CaMa-Flood set-ups using the hydrological model PCR-GLOBWB and the LSM H-TESSEL show the lowest skill with ~~48~~19 and ~~52~~18 stations noting ~~positive~~ scores greater than 0.5 respectively. On the contrary, best performance is from the calibrated Lisflood set-ups with

15   ~~average station~~median scores across stations of 0.~~37~~56, 0.~~41~~63 and 0.~~53~~64 for runs forced with ERA-Interim Land, ~~ERA-5 and~~ the reforecasts and ERA-5 respectively. Such results are unsurprising given that the KGE was used as the objective function in the calibration algorithm of the Lisflood routing model.

In terms of spatial distribution, poorest performance is consistent for the majority of simulations at the Arapari (*55*), Boca Do Inferno (*56*) and Base Alalau (*61*) gauging stations located north of Manaus, at the Fazenda Cajupiranga gauge (*64*) in

20   the northernmost Branco catchment and at the Fontanilhas (*35*) and Indeco (*49*) stations in the south-eastern Brazilian Amazon (Fig. 2).

 In the south-eastern Amazon, particularly in the Madeira and Tapajos sub-basins, the quantity of existing or under construction dams is at its highest (Fig. 1b). Damming of rivers is known to have impacts on different aspects of the flow regime with possible alterations in the timing, magnitude and frequency of low and high flows (Magilligan & Nislow, 2005).

25   Indeed, the frequency and duration of low and high flow pulses at stations downstream of dams has been shown to be particularly affected by the construction of cumulative dams (Timpe & Kaplan, 2017). Thus, discrepancies between observed modelled ~~and observed~~ data shown in Fig. 2 could be due to alterations to key features of the flow regime.

Highest scoring stations (KGE score > 0.~~7~~75) are predominately found in the south-western Brazilian Amazon where the network of tributaries remain relatively unaffected by damming~~.~~ and where slopes are gentle (Figs. 1b, d). However, high

30   skill at stations (*32*, *33* & *43*) along the Madeira river for most simulations (Fig. 2) highlight that the impacts of hydroelectric

dams needs to be considered on an individual basis with two of the largest dams (> 3000 MW) situated along the river (see Fig. 1b).

Figures 3, 4 and 5 show the breakdown of the KGE scores for each hydrological component to evaluate differences in performance with respect to the correlation (i.e. timing), flow variability (α) and bias ratio (β). An average of 79% of stations note correlation coefficients exceeding 0.6 across all runs with those using the Lisflood routing model performing similarly in both spatial distribution and magnitude (Fig. 3). In contrast, 51% and 47% of stations achieve values exceeding 0.6 for CaMa-Flood H-TESSEL and CaMa-Flood PCR-GLOBWB respectively, with the hydrological model, PCR-GLOBWB noting better performance at stations along the main-stem. The increased performance of Lisflood relative to simulations incorporating CaMa-Flood are likely due to the increased spatial resolution of the routing component (see Table 1). This is supported by results for CREST EF5, with 76% of stations noting values above 0.6 ~~with the~~ and the model occupying a finer spatial resolution ~~again much higher~~ than that of the CaMa-Flood ~~routing scheme~~ (Fig. 3g).

The variance of modelled river flow is on average higher than the observed time series in all of the simulations with the exception of the ERA-Interim Land PCR-GLOBWB CaMa-Flood simulation. For this run, 85% of stations observe values of less than one with stations situated in the Peruvian Amazon (*2, 3, 4* and *5*) the notable exception (Fig. 4b). In contrast, 79% of stations for the CaMa-Flood set-up using the LSM H-TESSEL, note values greater than one (Fig. 4a).

All runs tend to underestimate river flows relative to the observed time series with the majority of stations observing a beta value ~~below~~ of less than one (Fig. 5). ~~Almost half of all stations using~~ In the calibrated Lisflood ~~routing model~~ simulation forced with the reforecasts ~~achieve~~, almost half of all stations observe scores between 0.9 and 1.1 (i.e. grey circles~~) with the average between stations being exactly one~~), with a median of 0.99 (Table 2). These results are not replicated in the other two calibrated ~~simulations~~ runs when using either ERA-Interim Land or ERA-5 as the precipitation input (Figs. 5d & 5f~~) with a~~). For both of these runs a decrease is found in the number of stations ~~observing~~ achieving scores between 0.9 and 1.1 relative to the associated uncalibrated Lisflood set-ups (Figs. 5c & 5e). This is also highlighted by a decrease in the median scores of the two respected runs (Table 2), meaning that a greater water deficit exists in the calibrated set-ups.

Stations in the south-eastern Amazon, particularly in the upper reaches of the Teles Pires river (*37, 38 & 49*), tend to underestimate river flow for most simulations (Fig. 5). In this region of the basin precipitation is controlled by frontal systems in the South Atlantic Convergence Zone (SACZ~~)~~); which is prevalent during austral summer (Ronchail et al., 2002; Espinoza et al., 2009). In addition, rainfall variability in the Amazon is strongest in the south-east with a distinct dry season (Paiva et al., 2012; Espinoza et al., 2009). Further analysis could be useful in evaluating seasonal patterns of model performance to establish whether climatological features such as the SACZ are accurately represented within the precipitation datasets. Other factors impacting performance in the south east could be associated with the geology and topography (Figs. 1c, d). Stations in this area of the basin are located within the Brazilian Shields, composed predominately of Precambrian rock and are characterised by gentle slopes and low erosion rates (Filizola and Guyot, 2009). Paiva et al.

(2012) demonstrated the importance of accurate initial conditions of groundwater state variables in Tapajos and Xingu river basins, particularly for low flows. In comparison, the majority of the central parts of the basin are characterised by tertiary rocks, flat terrain, large floodplains and high sediment yields. In these regions (e.g. the south-western Brazilian Amazon), KGE scores are generally higher (Fig. 2), with surface water variables (e.g. water levels, surface runoff and floodplain storage) considered more important in hydrological prediction uncertainties (Paiva et al., 2012).

The KGE allows us to make explicit interpretations into the hydrological performance of each model owing to decomposition into correlation, bias and variability terms (Kling et al., 2012). The results indicate that the required developments to improve the representation of daily river flows is specific to each individual model and to the area of interest. For instance, for the ERA-Interim Land PCR-GLOBWB run, daily correlation scores (Fig. 3b) showed the model suffers at reproducing the temporal dynamics of flow (as measured by r) in northern catchments. Calibration of parameters which control the timing of the flood wave (e.g. river flow velocity) may improve performance. Whereas, model set-ups incorporating the uncalibrated Lisflood routing model generally had lower KGE values in the east of the basin corresponding to an overestimation of river flow variability (Figs. 2c & 4c, e). For these runs, performance slightly improved upon the calibration of the groundwater and routing parameters relating to timing, flow variability and groundwater loss (Figs. 2d & 4d, f).

3.2 Which model set-up best represents annual maximum river flows?

Both the calibrated and uncalibrated versions of Lisflood simulations forced with the ERA-5 datasetreanalysis are the best performing runs with average correlation coefficientsmedian scores of 0.4853 and 0.54 for boththe uncalibrated and calibrated simulations respectively (Fig. 7 & Table 2). However, a large deterioration in skill is evident for all simulations for Spearman's ranked coefficients between observed and predicted annual maximum river flows (Fig. 6) with only 21% of stations on average observing scores exceeding 0.6 across all simulations. Here, it is important to note that due to the length of some station time series the number of overlapping data points can be small and therefore the spatial distribution of model performance should be interpreted with caution. To provide a certain level of confidence between results, stations whose time series equals or exceeds 15 years are denoted using a circle, whereas those between 10-14 and 5-9 are represented using a square and triangle respectively.

Highest scores are generally located towards the eastern side of the basin aroundand along the mouth of themain Amazon River, though these where the terrain is predominately flat, and rivers drain extensive floodplains. These are constrained to runs using the Lisflood routing model with either ERA-Interim Land or ERA-5 as forcing (FigFigs. 6c-f). Interestingly, the calibrated Lisflood set-up forced using the reforecasts does not replicate scoresgood performance in this regionthese regions (Fig. 6h)., indicating that the error between simulated and observed peak river flows could be associated with the precipitation. When observing daily mean precipitation totals over the validation period (1997-2015), the reforecasts observe lower precipitation totals over central to northern areas of the basin relative to both of the climate reanalysis datasets (Fig. 8).

However, when comparing the results of ERA-Interim Land H-TESSEL CaMa-Flood and the ERA-Interim Land H-TESSEL Lisflood_uc set-ups, correlations are much lower in the CaMa-Flood simulation, suggesting that both precipitation and routing processes are equally important (Figs. 6a & 6c).

Low agreement between peaks is consistent in the south-east and north-west of the basin across all simulations (Fig. 6). In the south-east, a lack of skill could again be associated with the abundance of hydroelectric dams in the region or through the poor representation of the SACZ rainfall regime. Evaluating the ability to represent the timing and magnitude of the annual flood wave has important implications for models predicting flood hazard and for practices providing early warning information. These results identify that while the representation of daily river flows improves upon model calibration of the Lisflood routing model (Sect. 3.1), the influence of routing calibration for simulating flood peaks has no impact.

3.3 What is the best performing hydrological routing model?

We assessed the performance of the CaMa-Flood and Lisflood_uc routing models by comparing the two runs which are forced using the ERA-Interim Land reanalysis dataset. On average the uncalibrated Lisflood run outperforms CaMa-Flood for all metrics analysed with the exception of the bias ratio component of the KGE (Table 2).(Fig. 7 & Table 2). Results from the EF5 CREST model are also discussed but are not directly comparable due to differing meteorological inputs.

Scores fromThe median score of the correlation component of the KGE are(i.e. Pearson's correlation coefficient) is found to increase on average by 0.1819 when using the un-calibrated Lisflood model relative to CaMa-Flood with 28 more stations achieving a correlation score of 0.6 or higher (Figs. 3a & c). This number increases when considering correlation scores greater than 0.8 with 38 and seven stations reaching this value for Lisflood and CaMa-Flood respectively. The most notable increase in skill is found in Peru along the Marañón and Napo rivers (*2 & 5*)), which note an increase of 0.85 and 0.71 respectively when using the Lisflood model. In comparison, the EF5 CREST simulation fits between the CaMa-Flood and Lisflood runs with an averagea median daily correlation score of 0.65 while71 and notes 12 stations achievewhich have scores greater than 0.8 (Fig. 3g).

For the overall KGE metric, 6924% and 3% of stations have positive values exceeding 0.5 and 0.75 for CaMa-Flood and 24% are found to exceed 0.5.. These figures rise to 83% and 52% and 11% respectively in the uncalibrated Lisflood run. Large differences are particularly notable at stations situated in the upper reaches of the Solimões River (*2-6*) and within a cluster of stations situated towards the Colombian Amazon in the north-west (Fig. 2c). Results from the EF5 CREST model again fit between CaMa-Flood and Lisflood with 77% and 40% of stations exceeding zero and 0.5 respectively and a median score close to that of Lisflood (Fig. 7c). Larger differences are identified for peak flow correlations with only three stations (*27*, *17* and *22*) achieving scores exceeding 0.6 for the CaMa-Flood simulation compared to 22 using the uncalibrated Lisflood routing scheme (Figs. 6a & 6c). In comparison, the CREST EF5 simulation has 11 stations exceeding this threshold

with no distinguishable pattern (Fig. 6g). For this run, the time series of modelled data is shorter (2004-2015) and so peak flow correlations should be interpreted with caution.

Stations located in and around the main Amazon River observe better performance for representing flood peaks in the Lisflood simulation (Fig. 6c), aligning with the locations of lakes included within the Lisflood set-up (see Zajac et al., 2017). This level of skill was not replicated in the CaMa-Flood simulation where the representation of lakes is not included (Fig. 6a), suggesting the potential importance of lake parameterisation for accurate peak flow estimations. However, Zajac et al. (2017) demonstrated that although the inclusion of lakes in Lisflood was found to generally improve the representation of extreme discharge for the five and twenty year return periods on the global domain, the change in skill upon the inclusion of lakes and reservoirs in the Amazon was minimal for several metrics. Very few reservoirs are included within Lisflood in the Amazon and therefore the estimated effects on simulated streamflow is restricted.

Zhao et al. (2017) concluded the importance in the choice of different river routing ~~scheme~~schemes for simulating peak discharge across the globe ~~while~~. While Hoch et al. (2017b) comparison of two routing models found results to differ despite having identical boundary conditions. It is therefore of interest to evaluate not only the entire GHM set-up but also to assess the suitability of each model component of the hydrological chain in order to determine which routing model is most suitable for certain applications within the Amazon basin. ~~Differences in skill for the KGE results is likely associated to the correlation (i.e. timing) with a similar mean and median for the variability and bias ratio (Table 2 and Fig. 7). This suggests that adjustments of~~Results suggests that adjustments of certain parameters such as the Manning's channel coefficient could potentially improve the performance of the CaMa-Flood model, with the default coefficient higher in the uncalibrated Lisflood set-up (0.10 as opposed to 0.03; see Hirpa et al., 2018 for all default parameter values).

3.4 What is the best performing precipitation dataset?

Three precipitation products (ERA-Interim Land, ERA-5 and the reforecasts) are used to force the calibrated Lisflood routing model with the most recent ERA-5 reanalysis product the best performing dataset. Figure 8 displays the mean daily precipitation for each dataset over the main validation period (1997-2015). Main differences can be seen in the far west of the basin towards the Andes mountains, where precipitation is higher in ERA-5 compared to ERA-Interim Land and in the north-west where average daily precipitation totals are smaller in the reforecasts. On the other hand, values in the south-eastern corner of the basin are very similar between the three datasets. When comparing observed and simulated annual peak flows, median correlation scores improve by ~~an average of~~ 0.~~11~~12 and 0.~~15~~22 when using ERA-5 compared to using ERA-Interim Land and the reforecasts respectively (Table 2). 28 stations reach the 0.6 threshold ~~compared~~relative to 22 and nine stations for ERA-Interim Land and the reforecasts respectively with the range of coefficients smaller for ERA-5 (Fig. 7a).

Figures ~~8e~~9e and ~~8f~~9f highlight the relative gain or loss in skill when using ERA-5 compared to ERA-Interim Land. Greatest improvements for each metric are observed within the upstream reaches of the Solimões River, particularly for stations

15

located within the Peruvian Amazon (*2, 4 & 5*). In the main western headwater to the Solimões River (the Marañón river) at the San Regis gauging site (*2*) and at Tamshiyacu (*4*) near to the city of Iquitos, the annual maximum correlation skill scores are 0.51 and 0.59 respectively. These results highlight that poor performance found in upstream reaches of the Solimões River (Fig. 6c & 6d) is likely due to the representation of rainfall rather than routing performance.

5 In the other main tributary to the Solimões River, the Ucayali river, simulated annual peak flows show little agreement with observed data with a decrease in skill identified when using ERA-5 as opposed to ERA-Interim Land (Fig. 8e9e). Despite the lack of agreement between observed and modelled data in the Ucayali river, the higher correlation scores identified downstream at Tamshiyacu suggests that better representation of high-water periods at the start of the Solimões River is likely modulated by the larger Marañón river. Therefore, ~~our~~the ability to represent flood hazard in communities near to the
10 city of Iquitos is more dependent on how well we can predict river flow in the Marañón river.

All three runs perform well for the KGE metric with little difference in results spatially~~.~~ (Figs. 2d, f, h). The reforecast ~~run~~simulation used within the Lisflood calibration is found to be ~~slightly~~ superior with ~~91~~75% of stations achieving scores ~~above zero~~ which exceed 0.5 relative to ~~88% with~~71% and 59% for ERA-5 and ERA-Interim Land ~~and ERA-5. Differences between ERA-Interim Land and ERA-5 become more evident when observing scores exceeding higher thresholds with nine~~
15 ~~more stations scoring above 0.5 for ERA-5.~~respectively. Increased skill in the Peruvian Amazon is again the most noteworthy (Fig. 8f9f) with KGE skill scores of 0.67 for the Requena (*3*) (Ucayali river) and San Regis (*2*) (Marañón river) stations and 0.71 for Tamshiyacu (*4*) (Solimões River) when using ERA-5 relative to ERA-Interim Land. This increase in KGE skill can be attributed to an improvement in the variability and bias ratios found between the simulated and observed time series. Daily correlation scores for the three stations (*2, 3 & 4*) are near identical with the variance and bias ratios
20 underestimated for ERA-Interim Land, while being much closer to the observed data for ERA-5 (Figs. 4d, f & 5d, f).

The Tamshiyacu gauging station (*4*) is used to measure flood hazard in the city of Iquitos at the start of the Solimões River (Espinoza et al., 2013) and is therefore of particular interest. At this important location, scatterplots of observed against simulated river discharge (Fig. 910) show that the negative bias observed when using ERA-Interim Land ~~reanalysis~~ is corrected when using ERA-5, with the magnitude of the 90th percentile of river flows almost identical to that of the observed
25 dataset. Improvement is likely associated with the increased resolution of the ERA-5 reanalysis~~.~~, which observes higher daily mean precipitation totals in regions towards the Andes in the far north west of the basin (Fig. 8b). Waters found at Tamshiyacu are of Andean origin meaning that the representation of rainfall in the Andes Mountains is fundamental to accurately predicting streamflow. ERA-5 runs at a horizontal resolution of ~~~32~~31 km and includes an additional 73 vertical levels to 0.01 hPa compared to ERA-Interim Land, meaning the representation of the troposphere is enhanced~~.~~ (ECMWF,
30 2017).

The success of GHMs in producing adequate estimates of river flow is underpinned by uncertainties within the meteorological input (Butts et al., 2004; Beven, 2012; Sood & Smakhtin, 2015). These results have particular importance for

16

flood forecasting applications and research concerning extreme floods with the higher resolution ERA-5 dataset providing closer agreement between observed and simulated annual maximum river flows, particularly for the Peruvian Amazon. With the time series of observed data often beginning in the 1980's in the Amazon, ERA-5 could provide a useful tool for analysing historical flows and establishing links to climate variability. Upon completion, ERA-5 will date back to 1950

5   (Zsoter et al., ~~in review~~2019) meaning locations in which model skill is considered high could benefit from up to 30 years' worth of additional data for use in climate studies~~;~~ thus, allowing for more robust analysis. In future work, it could be of interest to compare the performance of ERA-5 against a wider range of precipitation data sets, such as the Multi-Source Weighted-Ensemble Precipitation (MSWEP) product that carefully integrates gauge, satellite and reanalysis based estimates. Beck et al. (2017) evaluation of 22 precipitation datasets previously demonstrated the advantages of using merged products

10   for hydrological modelling purposes.

3.5 How do results differ between using a LSM and a hydrological model?

The LSM~~,~~ H-TESSEL and the hydrological model~~,~~ PCR-GLOBWB ~~were~~are directly compared whereby the precipitation forcing (ERA-Interim Land) and river routing scheme (CaMa-Flood) ~~were~~are consistent. Overall, it appears that the choice between using a LSM or a hydrological model in the Amazon basin is dependent not only on the specific region of interest

15   but also on the application and needs of the user. Previous studies (Zhang et al., 2016; Beck et al., 2017) have found that LSM models, on average, perform better in rainfall dominant regions, whereas hydrological models tend to achieve better results in snow dominated regions owing to the use of complex energy balance equations introducing additional uncertainties. For the Amazon basin, ~~the average~~ Spearman's rank correlation coefficients between simulated and observed peak river flow ~~is slightly higher for the LSM~~are closely matched with ~~scores~~a median of 0.~~25~~24 and 0.~~19~~23 for H-TESSEL

20   and PCR-GLOBWB respectively (Table 2). However, the number of stations with Spearman's maximum correlation scores exceeding 0.6 is slightly higher in PCR-GLOBWB at ~~nine~~seven compared to ~~just~~ three with H-TESSEL (Figs 6a & 6b).

To illustrate the gain or loss in skill when using the LSM relative to PCR-GLOBWB the Spearman's annual maximum correlation and KGE skill scores were calculated for each station (Figs. ~~8g & 8h~~9g & 9h). Overall, 68% of stations show improved skill for peak river flow correlations when using the LSM model, though the ~~average~~ gain in skill is minimal

25   (~~mean~~median correlation skill score = 0.~~03~~06). This percentage drops to 37% and 22% for improvements in skill which ~~exceed~~exceeds 0.1 and 0.2 respectively (Fig. ~~8g~~9g). On the contrary, over half of stations see improvements for the KGE skill score for the hydrological model, PCR-GLOBWB and 23% of stations observe KGE skill score increases exceeding 0.25 (Fig. ~~8h~~9h).

A large loss in performance for the KGE can be seen when using H-TESSEL at stations in the Peruvian Amazon at the

30   confluence point to the Solimões River with PCR-GLOBWB CaMa-Flood noting similar scores to the calibrated version of the Lisflood routing model at the San Regis (*2*) and Tamshiyacu (*4*) gauging sites (Fig. ~~8h~~9h). These stations have KGE skill scores of -4.02 and -1.11 respectively. Model performance in this region can largely be attributed to the failure of the H-

17

TESSEL CaMa-Flood run to accurately represent the variance of flow and the temporal correlation component of the KGE with the variability of modelled flow far higher than in the observed data (Fig. 4a). Northern regions in the Branco basin and stations situated towards the Colombian Amazon show the opposite effect with higher KGE coefficients found for the H-TESSEL CaMa-Flood run~~,~~ (Fig. 2a), indicating that model suitability is regionally specific.

5 **3.6 By how much does the calibration of groundwater and routing parameters improve performance?**

Calibration of hydrological models is known to be a useful tool in providing more accurate estimates of river flow (Beck et al., 2017). However, due to a lack of data and the computational expense required in the calibration of GHMs, many remain uncalibrated (Bierkens, 2015; Sood & Smakhtin, 2015). Both Gupta et al. (2009) and Mizukami et al. (2019) demonstrate that square error type metrics are unsuitable for model calibration when the model in question requires robust performance
10 for high river flows. Improvement of flow variability estimates was documented in both studies when switching the calibration metric from the NSE to the KGE for both a simple rainfall-runoff model (similar to the HBV model; Bergström, 1995) and for two more complex hydrological models (VIC and mHM), suggesting similar results are likely to be achieved for other hydrological models. To investigate the potential benefits of routing model calibration, whereby the KGE was used as the objective function, the time series of river discharge for the calibrated Lisflood runs forced using the ERA-Interim
15 Land and ERA-5 reanalysis datasets were compared against the associated default set-ups without routing calibration.

Overall, hydrological performance~~, on average,~~ improves upon model parameter calibration with ~~computed~~positive KGE skill scores ~~for both~~ (i.e. an increase in skill) at 61% (59%) of gauging stations for simulations forced with ERA-Interim Land ~~and~~ (ERA-5~~increasing on average by 0.13 and 0.14 respectively.~~) (Figs. 9c & 9d). The influence of calibration is ~~found to be similar between precipitation datasets~~stronger for the simulation forced with ERA-5, with the number of stations
20 ~~considered skillful for the~~achieving "intermediate" KGE ~~upon calibration~~scores (i.e. 0.75 > KGE ⩾ 0.5) totalling ~~66~~53 compared to 43 for ~~both the~~ERA-Interim Land ~~and ERA-5 simulations~~, an increase of ~~two~~nine and ~~four~~12 stations ~~respectively~~relative to the associated uncalibrated runs. When observing the spatial distribution of relative improvements, an east/west divide can be seen (Figs. ~~8c & 8d~~9c & 9d). Generally, decreases in skill are concentrated to stations in the western side of the basin, whereas stations located to the east display improved hydrological representation.

25 Three stations (*2, 3 & 4*) in the Peruvian Amazon show increased KGE skill scores when using the calibrated ERA-5 run relative to the similar uncalibrated set-up (Fig. ~~8d~~9d). Conversely, a loss in skill is observed at each station for the calibrated run forced using ERA-Interim Land (Fig. ~~8c~~9c). These results are likely associated to a larger negative runoff bias within the ERA-Interim Land Lisflood_uc run relative to the ERA-5 Lisflood_uc simulation (Figs. 5c and 5e) for the three stations. This is supported by Hirpa et al. (2018~~)~~), who concluded that stations which have a negative streamflow bias in the default
30 run (i.e. Lisflood_uc) also have a negative KGE skill score in the calibrated simulation owing to the challenge of correcting for a water deficit within the routing component. Thus, for GHMs which tend to underestimate runoff, adjustments of parameters within the LSM or hydrological model (e.g. those responsible for the portioning of precipitation into runoff) or

18

through bias correction measures within the precipitation dataset, may be advantageous in efforts to accurately represent floods.

No significant differences between calibrated and uncalibrated Lisflood annual maximum correlation scores are identified between simulated and observed peaks (Fig. 77a & Table 2). In total, the number of stations exceeding the 0.6 threshold for peak flow correlations remains the same for runs involving ERA-5 and decreases by one for ERA-Interim Land, meaning that the routing model calibration has very little impact on ourin the ability to capture annual peaks, with the precipitation dataset used to force the LSM more influential. This suggests that calibrated parameters controlling flow timing (e.g. Manning's channel coefficient) are not as important for simulating the magnitude of higher flows in the Amazon basin and that bias correction of the precipitation or calibration of parameters associated with runoff and evapotranspiration might be more useful. As previously highlighted by Hirpa et al. (2018)), the inclusion of an objective function that is explicitly based on flood peaks could improve the ability of Lisflood to simulate floods. This is supported by previous studies (Greuell et al., 2015; Beck et al., 2017; Mizukami et al., 2019) which have also identified that improved performance in calibrated models is predominately specific to metrics which are incorporated into the objective function used within the calibration. For instance, in Mizukami et al. (2019) they find that when using an application specific metric (Annual Peak Flow Bias; APFB) for the calibration of two hydrological models, it produced the best peak flow annual estimates compared to using the NSE, KGE and its components. However, despite this improvement, flood magnitudes were still underestimated for all metrics used in calibration and the use of the APFB as the calibration metric resulted in poorer performance across the individual KGE components upon evaluation.

3.7 Aspects forLimitations and future work

While estimating the magnitude of peak river flowflows is fundamental, more evaluation is required in assessing the ability to represent the timing of flood peaks. Flood Modelled flood peaks canhave been known to occur too early in large Amazonian rivers (Alfieri et al., 2013; Hoch et al., 2017b), but) with accurate flow timing is of particularsignificant importance toin the Amazon basin with. For example, the time displacement between peak flows in coinciding tributaries are known to play a major factorrole in the dampening of the Amazon flood wave (Tomasella et al., 2010) and in the synchronisation of flood peaks, commonly associated with exceptional flood events throughout the Amazon basin (e.g. Marengo et al., 2012; Espinoza et al., 2013; Ovando et al., 2016). Additional evaluation using metrics which focus specifically on the timing aspect, such as the delay index (Paiva et al., 2013), would enable a more complete assessment of the hydrological modelling regime.

A limitation of this type of study is due to the intercomparison being restricted to the macroscale (i.e. only a subset of potential modelling configurations are considered). In future work it would be useful to increase the granularity of the modelling decision matrix to allow conclusions to be more generalised across the modelling community. For instance, when comparing the performance of the Lisflood and CaMa-Flood routing models, the results are specific to the simulations forced

using the ERA-Interim Land reanalysis dataset. Although useful in providing a general indication of routing performance for each model when using a climate reanalysis dataset, the conclusions are specific to that particular comparison with differing results possible when using another precipitation input. Future work could investigate one of the research questions stated in the objectives (Sect 1.5) at a finer resolution. For example, comparing the Lisflood and CaMa-Flood routing models by

5   evaluating several runs which use a greater variety of precipitation products (e.g. MSWEP, CHIRP V2.0, ERA-5, TRMM v.7 amongst others) to force each model. Such analysis would allow more general conclusions and recommendations to be made to the modelling community who are interested in those particular routing schemes. A similar approach could be adopted for the assessment of other components of the hydrological modelling chain.

4 Conclusions

10   In this paper, eight different GHMs were employed in an intercomparison analysis using two verification metrics to assess model performance against gauged river discharge observations. The motivation for this work stemmed from the need to evaluate the ability of GHMs to reproduce historical floods in the Amazon basin for use in climate analysis and to identify the strengths and weaknesses which exist along the hydrological modelling chain in order to provide insight to model developers. The implications of these results suggest that the choice of precipitation dataset is the most influential

15   component of the GHM set-up in terms of our ability to recreate annual maximum river flows in the Amazon basin. This is evident with average station correlations between observed and simulated annual maximum river flows increasing when using the new ERA-5 reanalysis dataset with significant improvements in locations of the Peruvian Amazon. , with significant improvements in locations of the Peruvian Amazon. In this region, waters are sourced from Andean origins where rainfall can often be poorly represented due to topographically complex terrains (Paiva et al., 2013). Thus, those wishing to

20   simulate higher flows in the upper reaches of the Amazon may benefit from choosing a precipitation dataset which has a high spatial resolution, whereby the upper atmosphere is discretised at finer scales. Although, an exact recommended spatial resolution cannot be provided based on the results of this study alone, previous works (e.g. Beck et al., 2017) support the need for a comparatively high-resolution data set in addition to other advantageous factors such as a long temporal record and the inclusion of daily gauge corrections.

25   Although parameter calibration of the Lisflood routing model improved the representation of the whole hydrological regime across the basin, the agreement between observed and simulated peak discharge values saw no change upon the calibration. This indicates that the benefit of calibration is confined to the objective function used, in this case the KGE, and highlights that further model calibration should be undertaken using an objective function that fits the purpose of the application (e.g. RMSE of flood peaks or APFB for flood forecasting systems).) could be worth considering. It is important to reiterate

30   however, that thoughtful consideration is required if choosing application specific metrics, with the potential to degrade performance in other aspects of the hydrological regime (e.g. bias and flow variability ratios) a concern (Mizukami et al.,

20

References

Alfieri, L., Burek, P., Dutra, E., Krzeminski, B., Muraro, D., Thielen, J., and Pappenberger, F.: GloFAS-global ensemble streamflow forecasting and flood early warning, Hydrol. Earth Syst. Sci., 17, 1161, https://doi.org/10.5194/hess-17-1161-2013, 2013.

Alfieri, L., Cohen, S., Galantowicz, J., Schumann, G. J., Trigg, M. A., Zsoter, E., Prudhomme, C., Kruczkiewicz, A., Coughlan de Perez, E., Flamig, Z., Rudari., R., Wu, H., Adler, R. F., Brakenbridge, R. G., Kettner, A., Weerts, A., Matgen, P., Islam, S. A. K. M., and Salamon, P.: A global network for operational flood risk reduction, Environ. Sci. Policy., 84, 149-158, https://doi.org/10.1016/j.envsci.2018.03.014, 2018.

Andreadis, K. M., Schumann, G. J. P., Stampoulis, D., Bates, P. D., Brakenridge, G. R., and Kettner, A. J.: Can Atmospheric Reanalysis Data Sets Be Used to Reproduce Flooding Over Large Scales?, Geophys. Res. Lett., 44, 10369-10377, https://doi.org/10.1002/2017GL075502, 2017.

Arnell, N. W., and Gosling, S. N.: The impacts of climate change on river flood risk at the global scale, Clim. Change., 134, 387-401, https://doi.org/10.1007/s10584-014-1084-5, 2016.

Arnold, J. G., Srinivasan, R., Muttiah, R. S., and Williams, J. R.: Large area hydrologic modeling and assessment part I: model development 1, J. Am. Water Resour. Assoc., 34, 73-89, 1998.

Balsamo, G., Beljaars, A., Scipal, K., Viterbo, P., van den Hurk, B., Hirschi, M., and Betts, A. K.: A revised hydrology for the ECMWF model: Verification from field site to terrestrial water storage and impact in the Integrated Forecast System, J. Hydrometeorol., 10, 623-643, https://doi.org/10.1175/2008JHM1068.1, 2009.

Balsamo, G., Pappenberger, F., Dutra, E., Viterbo, P., and Van den Hurk, B. J. J. M.: A revised land hydrology in the ECMWF model: a step towards daily water flux prediction in a fully-closed water cycle, Hydrol. Process., 25, 1046-1054, https://doi.org/10.1002/hyp.7808, 2010.

Balsamo, G., Albergel, C., Beljaars, A., Boussetta, S., Brun, E., Cloke, H.., Dee, H., Dutra, D., Muñoz-Sabater, J., Pappenberger, F., de Rosnay, P., Stockdale. T., and Vitart, F.: ERA-Interim/Land: a global land surface reanalysis data set, Hydrol. Earth Syst. Sci., 19, 389-407, https://doi.org/10.5194/hess193892015, 2015.

Beck, H. E., van Dijk, A. I., de Roo, A., Dutra, E., Fink, G., Orth, R., and Schellekens, J.: Global evaluation of runoff from ten state-of-the-art hydrological models, Hydrol. Earth Syst. Sci., 21, 2881-2903, https://doi.org/10.5194/hess-21-2881-2017, 2017.

Balsamo, G., Agusti-Panareda, A., Albergel, C., Arduini, G., Beljaars, A., Bidlot, J., Bousserez, N., Boussetta, S., Brown, A., Buizza, R., Buontempo, C., Chevallier, F., Choulga, M., Cloke, H., Cronin, M. F., Dahoui, M., De Rosnay, P., Dirmeyer, P. A., Drusch, M., Dutra, E., Ek, M. B., Gentine, P., Hewitt, H., Keeley, S. P. E., Kerr, Y., Kumar, S., Lupu, C., Mahfouf, J. F., McNorton, J., Mecklenburg, S., Mogensen, K., Muñoz-Sabater, J., Orth, R., Rabier, F., Reichle, R., Ruston, B, Pappenberger, F., Sandu, I., Seneviratne, S. I., Tietsche, S., Trigo, I. F., Uijlenhoet, R., Wedi, N., Woolway, R. L., & Zeng, X.: Satellite and In Situ Observations for Advancing Global Earth Surface Modelling: A Review. Remote Sens., 10, 2038, https://doi.org/10.3390/rs10122038, 2018.

Beck, H. E., Vergopolan, N., Pan, M., Levizzani, V., van Dijk, A. I., Weedon, G. P., Brocca, L., Pappenberger, F., Huffman, G. J., & Wood, E. F.: Global-scale evaluation of 22 precipitation datasets using gauge observations and hydrological modeling, Hydrol. Earth Syst. Sci., 21, 6201-6217, https://doi.org/10.5194/hess-21-6201-2017, 2017.

Bergström, S.: The HBV model, in: Comput. Model. Watershed Hydrol., edited by Singh, V., chap. The HBV mo, Water Resouces Publications, Highlands Ranch Co., 1995.

Beven, K. J.: *Rainfall-Runoff Modelling: The Primer*, 2nd ed., Wiley-Blackwell, Chichester, U.K, 2012.

Bierkens, M. F.: Global hydrology 2015: State, trends, and directions, Water Resour. Res., 51, 4923-4947., https://doi.org/10.1002/2015WR017173, 2015.

Bierkens, M. F., Bell, V. A., Burek, P., Chaney, N., Condon, L. E., David, C. H., de Roo, A., Döll, P., Drost, N., Famigiletti, J.S., Flörke, M., Gochis, D. J., Houser, P., Hut, R., Keune, J., Kollet, S., Maxwell, R. M., Reager, J. T., Samaniego, L., Sudicky, E., Sutanudiaia, E. H., van de Giesen, N., Winsemius, H., and Wood, E. F.: Hyper-resolution global hydrological modelling: what is next? "Everywhere and locally relevant", Hydrol. Process., 29, 310-320, https://doi.org/10.1002/hyp.10391, 2015.

Bondeau, A., Smith, P. C., Zaehle, S., Schaphoff, S., Lucht, W., Cramer, W., Gerten, D., Lotze-Campen, H., Muller, C., ¨ Reichstein, M., and Smith, B.: Modelling the role of agriculture for the 20th century global terrestrial carbon balance, Global Change Biol., 13, 679–706, https://doi.org/10.1111/j.1365- 2486.2006.01305.x, 2007.

Butts, M. B., Payne, J. T., Kristensen, M., and Madsen, H.: An evaluation of the impact of model structure on hydrological

5   modelling uncertainty for streamflow simulation, J. Hydrol., 298, 242-266, https://doi.org/10.1016/j.jhydrol.2004.03.042, 2004.

Clark III, R. A., Flamig, Z. L., Vergara, H., Hong, Y., Gourley, J. J., Mandl, D. J., Frye, S., Handy, M., and Patterson, M.: Hydrological modeling and capacity building in the Republic of Namibia, Bull. Am. Meteorol. Soc., 98, 1697-1715, https://doi.org/10.1175/BAMS-D-15-00130.1, 2016.

10   Correa, S. W., de Paiva, R. C. D., Espinoza, J. C., and Collischonn, W.: Multi-decadal Hydrological Retrospective: Case study of Amazon floods and droughts, J. Hydrol., 549, 667-684, https://doi.org/10.1016/j.jhydrol.2017.04.019, 2017.

Coughlan de Perez, E., van den Hurk, B. J. J. M., Van Aalst, M. K., Jongman, B., Klose, T., and Suarez, P.: Forecast-based financing: an approach for catalyzing humanitarian action based on extreme weather and climate forecasts, Nat. Hazards Earth Syst. Sci., 15, 895-904, https://doi.org//10.5194/nhess-15-895-2015, 2015.

15   De Groeve, T., Thielen-del Pozo, J., Brakenridge, R., Adler, R., Alfieri, L., Kull, D., Lindsay, F., Imperiali, O., Pappenberger, F., Rudari, R., Salamon, P., Villars, N., and Wyjad, K.: Joining forces in a global flood partnership, Bull. Am. Meteorol. Soc., 96, ES97-ES100, https://doi.org/10.1175/BAMS-D-14-00147.1, 2015.

Dee, D. P., Uppala, S. M., Simmons, A. J., Berrisford, P., Poli, P., Kobayashi, S., Andrae, U., Balmaseda, M.A., Balsamo, G., Bauer, P., Bechtold, P., Belijaars, A.C.M., van de Berg, L., Bidlot, J., Bormann, N., Delsol, C., Dragani, R., Fuentes, M.,

20   Geer, A.J., Haimberger, L., Healy, S.B., Hersbach, S., Hólm, E.V., Isaksen, L., Kallberg, P., Köhler, M, Matricardi, M., McNally, A.P., Mong-Sanz, B.M., Morcrette, J.J., Park, B.K., Peubey, C., de Rosnay, P., Tavolato, C., Thèpaut, J.N., and Vitart, F.: The ERA-Interim reanalysis: Configuration and performance of the data assimilation system, Q. J. R. Meteorol. Soc., 137, 553-597, https://doi.org/10.1002/qj.828, 2011.

Devia, G. K., Ganasri, B. P., & Dwarakish, G. S.: A review on hydrological models, Aquatic Procedia., 4, 1001-1007.,

25   https://doi.org/10.1016/j.aqpro.2015.02.126, 2015.

Döll, P., Kaspar, F., and Lehner, B.: A global hydrological model for deriving water availability indicators: model tuning and validation, J. Hydrol., 270, 105-134, https://doi.org/10.1016/S0022-1694(02)00283-4, 2003.

ECMWF.: A brief description of reforecasts: https://confluence.ecmwf.int/display/S2S/A+brief+description+of+reforecasts, last access: 25 September 2018, 2016.

30   ECMWF.: What are the changes from ERA-Interim to ERA5?: https://confluence.ecmwf.int//pages/viewpage.action?pageId=74764925, Last access: 31st August 2018, 2017.

ECMWF.: What is ERA-5?: https://confluence.ecmwf.int/display/CKB/What+is+ERA5, last access: 8 October 2018.

Emerton, R. E., Stephens, E. M., Pappenberger, F., Pagano, T. C., Weerts, A. H., Wood, A. W., Salamon, P., Brown, J. D., Hierdt, N., Donnelly, C., Baughc C. A., and Cloke, H. L.: Continental and global scale flood forecasting systems, Wiley Interdiscip. Rev. Water, 3, 391-418, https://doi.org/10.1002/wat2.1137, 2016.

Emerton, R., Zsoter, E., Arnal, L., Cloke, H. L., Muraro, D., Prudhomme, C., Stephens, E.M., Salamon, P., and
5 Pappenberger, F.: Developing a global operational seasonal hydro-meteorological forecasting system: GloFAS v2. 2 Seasonal v1. 0, Geosci. Model Dev., 11, 3327-3346, https://doi.org/10.5194/gmd-11-3327-2018, 2018.

Espinoza, J. C., Ronchail, J., Guyot, J. L., Cochonneau, G., Naziano, F., Lavado, W., De Oliveria, E., Pombosa, R., and Vauchel, P.: Spatio-temporal rainfall variability in the Amazon basin countries (Brazil, Peru, Bolivia, Colombia, and Ecuador), Int. J. Climatol., 29, 1574-1594, https://doi.org/10.1002/joc.1791, 2009.

10 Espinoza, J. C., Ronchail, J., Frappart, F., Lavado, W., Santini, W., and Guyot, J. L.: The major floods in the Amazonas River and tributaries (western Amazon basin) during the 1970–2012 period: A focus on the 2012 flood, J. Hydrometeorol., 14, 1000-1008, https://doi.org/10.1175/JHM-D-12-0100.1, 2013.

Espinoza, J. C., Marengo, J. A., Ronchail, J., Carpio, J. M., Flores, L. N., and Guyot, J. L.: The extreme 2014 flood in south-western Amazon basin: the role of tropical-subtropical South Atlantic SST gradient, Environ. Res. Lett., 9, 124007,
15 https://doi.org/10.1088/1748-9326/9/12/124007, 2014.

Espinoza, J. C., Ronchail, J., Marengo, J. A., and Segura, H.: Contrasting North–South changes in Amazon wet-day and dry-day frequency and related atmospheric features (1981–2017), Clim. Dyn., 1-18, https://doi.org/10.1007/s00382-018-4462-2, 2018.

Filizola, N., & Guyot, J. L.: Suspended sediment yields in the Amazon basin: an assessment using the Brazilian national data
20 set, Hydrol. Processes, 23, 3207-3215., https://doi.org/10.1002/hyp.7394, 2009.

Forbes, R., Haiden, T., and Magnusson, L.: Improvements in IFS forecasts of heavy precipitation. Meteorology section of ECMWF newsletter No. 144., 21-26, https://doi.org/10.21957/jxtonky0, 2015.

Gilleland, M. E.: Package 'verification', http://cran.utstat.utoronto.ca/web/packages/verification/verification.pdf, last access 25 September 2018, 2015.

25 Gloor, M. R. J. W., Brienen, R. J., Galbraith, D., Feldpausch, T. R., Schöngart, J., Guyot, J. L., Espinoza, J. C., Llyod, J., and Phillips, O. L.: Intensification of the Amazon hydrological cycle over the last two decades, Geophys. Res. Lett., 40, 1729-1733, https://doi.org/10.1002/grl.50377, 2013.

Gosling, S. N., and Arnell, N. W.: Simulating current global river runoff with a global hydrological model: model revisions, validation, and sensitivity analysis, Hydrol. Processes, 25, 1129-1145, https://doi.org/10.1002/hyp.7727, 2011.

30 Gourley, J. J., Flamig, Z. L., Vergara, H., Kirstetter, P. E., Clark III, R. A., Argyle, E., Arthur, A., Martinaitis, S., Terti, G., Erlingis, J.M., Hong, Y., and Howard, K.W.: The FLASH Project: Improving the tools for flash flood monitoring and prediction across the United States, Bull. Am. Meteorol. Soc., 98, 361-372, https://doi.org/10.1175/BAMS-D-15-00247.1, 2017.

Greuell, J. W., Andersson, J., Donnelly, C., Feyen, L., Gerten, D., Ludwig, F., Pisacane, G., Roudier, P., and Schaphoff, S.: Evaluation of five hydrological models across Europe and their suitability for making projections under climate change Hydrol. Earth Syst. Sci. Discuss.12, 10289-10330, https://doi.org/10.5194/hessd-12-10289-2015, 2015.

Gudmundsson, L., Wagener, T., Tallaksen, L.M., and Engeland, K.: Evaluation of nine large-scale

5   hydrological models with respect to the seasonal runoff climatology in Europe, Water Resour. Res., 48, https://doi.org/10.1029/2011WR010911, 2012.

Gupta, H. V., Kling, H., Yilmaz, K. K., and Martinez, G. F.: Decomposition of the mean squared error and NSE performance criteria: Implications for improving hydrological modelling , J. Hydrol., 377, 80-91, https://doi.org/10.1016/j.jhydrol.2009.08.003, 2009.

10   Guse, B., Pfannerstill, M., Gafurov, A., Kiesel, J., Lehr, C., and Fohrer, N.: Identifying the connective strength between model parameters and performance criteria, Hydrol. Earth Syst. Sci., 21, 5663-5679, https://doi.org/10.5194/hess-21-5663-2017, 2017.

Haddeland, I., Clark, D. B., Franssen, W., Ludwig, F., VOß, F., Arnell, N. W., Bertrand, N., Best, M., Folwell, S., Gerten, D., Gomes, S., Gosling, S.N., Hagemann, S., Hanasaki, N., Harding, R., Heinke, J., Kabat, P., Koirala, S, Oki, T., Polcher, J.,

15   Stacke, T., Viterbo, P., Weedon, G.P., and Yeh, P.: Multimodel estimate of the global terrestrial water balance: Setup and first results, J. Hydrometeorol., 12, 869-884, https://doi.org/10.1175/2011JHM1324.1, 2011.

Hattermann, F. F., Krysanova, V., Gosling, S. N., Dankers, R., Daggupati, P., Donnelly, C., Flörke, M., Huang, S., Motovilov, Y., Buda, S., Yang, T., Müller, C., Leng, G., Tang, Q., Portmann, F. T., Hagemann, S., Gerten, D., Wada, Y., Masaki, Y., Alemayehu, T., Satoh, Y., and Samaniego, L.: Cross-scale intercomparison of climate change impacts simulated

20   by regional and global hydrological models in eleven large river basins, J. Clim. Change, 141, 561-576, https://doi.org/10.1007/s10584-016-1829-4, 2017.

Hirabayashi, Y., Mahendran, R., Koirala, S., Konoshima, L., Yamazaki, D., Watanabe, S., Kim, H., and Kanae, S.: Global flood risk under climate change, Nat. Clim. Chang., 3, 816, https://doi.org/10.1038/nclimate1911, 2013.

Hirpa, F. A., Salamon, P., Beck, H. E., Lorini, V., Alfieri, L., Zsoter, E., and Dadson, S. J.: Calibration of the Global Flood

25   Awareness System (GloFAS) using daily streamflow data, J. Hydrol., 566, 595-606, https://doi.org/10.1016/j.jhydrol.2018.09.052, 2018.

Hoch, J. M., Haag, A. V., Dam, A. V., Winsemius, H. C., van Beek, L. P., and Bierkens, M. F.: Assessing the impact of hydrodynamics on large-scale flood wave propagation–a case study for the Amazon Basin, Hydrol. Earth Syst. Sci., 21, 117-132, https://doi.org/10.5194/hess-21-117-2017, 2017a.

30   Hoch, J. M., Neal, J., Baart, F., van Beek, L. P. H., Winsemius, H., Bates, P., and Bierkens, M. F.: GLOFRIM v1. 0–A globally applicable computational framework for integrated hydrological–hydrodynamic modelling, Geosci. Model Dev., 10, 3913-3929, https://doi.org/10.5194/gmd-10-3913-2017, 2017b.

Huffman, G. J., Bolvin, D. T., Nelkin, E. J., Wolff, D. B., Adler, R. F., Gu, G., Hong, Y., Bowman, K.P., and Stocker, E. F.: The TRMM multisatellite precipitation analysis (TMPA): Quasi-global, multiyear, combined-sensor precipitation estimates at fine scales, J. Hydrometeorol., 8, 38-55, https://doi.org/10.1175/JHM560.1, 2007.

Huffman, G. J., Adler, R. F., Bolvin, D. T., and Gu, G.: Improving the global precipitation record: GPCP version 2.1,

5   Geophys. Res. Lett., 36, https://doi.org/10.1029/2009GL040000, 2009.

IFRC.: Disaster Relief Fund (DREF) Peru: Floods. https://reliefweb.int/sites/reliefweb.int/files/resources/MDRPE005du1.pdf, last access: 25 September 2018, 2013.

Kling, H., Fuchs, M., and Paulin, M.: Runoff conditions in the upper Danube basin under an ensemble of climate change scenarios, J. Hydrol., 424, 264-277, https://doi.org/10.1016/j.jhydrol.2012.01.011, 2012.

10   Latrubesse, E. M., Arima, E. Y., Dunne, T., Park, E., Baker, V. R., d'Horta, F. M., Wight, C., Wittmann, F., Zuanon, J., Baker, P. A., Ribas, C. C., Norgaard, R. B., Filizola, N., Ansar, A., Flyvbjerg, B., and Stevaux, J. C.: Damming the rivers of the Amazon basin. Nature, 546, 363, https://doi.org/10.1038/nature22333, 2017.

Legates, D. R., and McCabe, G. J.: Evaluating the use of "goodness-of-fit" measures in hydrologic and hydroclimatic model validation, Water Resour. Res., 35, 233-241, https://doi.org/10.1029/1998WR900018, 1999.

15   Lehner, B., Verdin, K., and Jarvis, A.: New global hydrography derived from spaceborne elevation data. Eos, Transactions American Geophysical Union, 89, 93-94, https://doi.org/200810.1029/2008EO100001, 2008.

Magilligan, F. J., and Nislow, K. H.: Changes in hydrologic regime by dams. Geomorphology, 71, 61-78, https://doi.org/10.1016/j.geomorph.2004.08.017, 2005.

Marengo, J. A., Tomasella, J., Soares, W. R., Alves, L. M., and Nobre, C. A.: Extreme climatic events in the Amazon basin,

20   Theor. Appl. Climatol., 107, 73-85, https://doi.org/10.1007/s00704-011-0465-1, 2012.

Marengo, J. A., Alves, L. M., Soares, W. R., Rodriguez, D. A., Camargo, H., Riveros, M. P., and Pabló, A. D.: Two contrasting severe seasonal extremes in tropical South America in 2012: flood in Amazonia and drought in northeast Brazil, J. Clim., 26, 9137-9154, https://doi.org/10.1175/JCLI-D-12-00642.1, 2014.2013.

Marengo, J. A., and Espinoza, J. C.: Extreme seasonal droughts and floods in Amazonia: causes, trends and impacts, Int. J.

25   Climatol., 36, 1033-1050, https://doi.org/10.1002/joc.4420, 20152016.

Meade, R. H., Rayol, J. M., Da Conceicão, S. C., and Natividade, J. R.: Backwater effects in the Amazon River basin of Brazil, Environ. Geol. Water Sci., 18, 105-114, https://doi.org/10.1007/BF01704664, 1991.

Meigh, J. R., McKenzie, A. A., and Sene, K. J.: A grid-based approach to water scarcity estimates for eastern and southern Africa, Water Resour. Mange., 13, 85-115, https://doi.org/10.1023/A:1008025703712, 1999.

30   Meng, J., Li, L., Hao, Z., Wang, J., and Shao, Q.: Suitability of TRMM satellite rainfall in driving a distributed hydrological model in the source region of Yellow River, J. Hydrol., 509, 320-332, https://doi.org/10.1016/j.jhydrol.2013.11.049, 2013.

Mizukami, N., Rakovec, O., Newman, A., Clark, M., Wood, A., Gupta, H., and Kumar, R.: On the choice of calibration metrics for high flow estimation using hydrologic models, Hydrol. Earth Syst. Sci. Discuss., https://doi.org/10.5194/hess-2018-391, 2019.

26

Mittermaier, M., Roberts, N., and Thompson, S. A.: A long-term assessment of precipitation forecast skill using the Fractions Skill Score, Meteorol. Appl., 20, 176-186, https://doi.org/10.1002/met.296, 2013.

Mundial Grupo Banco: http://bibliotecadigital.planejamento.gov.br/xmlui/bitstream/handle/iditem/658/Banco%20Mundial_~~opcoes~~opcoes-_de%20prote%C3%A7%C3%A3o%20financeira%20contra%20desastres%20no%20Brasil.pdf?sequence=1, last Access: 25 September 2018, 2014.

Nash, J. E., and Sutcliffe, J. V.: River flow forecasting through conceptual models part I—A discussion of principles , J. Hydrol., 10, 282-290, https://doi.org/10.1016/0022-1694(70)90255-6, 1970.

Novak, D. R., Bailey, C., Brill, K. F., Burke, P., Hogsett, W. A., Rausch, R., and Schichtel, M.: Precipitation and temperature forecast performance at the Weather Prediction Center, Weather Forecasting, 29, 489-504, https://doi.org/10.1175/WAF-D-13-00066.1, 2014.

Ovando, A., Tomasella, J., Rodriguez, D. A., Martinez, J. M., Siqueira-Junior, J. L., Pinto, G. L. N., Passy, P., Vauchel, P, Noriega, L., and von Randow, C.: Extreme flood events in the Bolivian Amazon wetlands., J. Hydrol.: Reg. Stud., 5, 293-308, https://doi.org/10.1016/j.ejrh.2015.11.004, 2016.

Paiva, R. C. D., Collischonn, W., Bonnet, M. P., & De Gonçalves, L. G. G. (2012). On the sources of hydrological prediction uncertainty in the Amazon, Hydrol. Earth Syst. Sci., 16, 3127-3137., https://doi.org/10.5194/hess-16-3127-2012, 2012.
Paiva, R. C. D., Buarque, D. C., Collischonn, W., Bonnet, M. P., Frappart, F., Calmant, S., and Mendes, C. A. B.: Large-scale hydrologic and hydrodynamic modeling of the Amazon River basin, Water Resour. Res., 49, 1226-1243, https://doi.org/10.1002/wrcr.20067, 2013.

Pappenberger, F., Dutra, E., Wetterhall, F., and Cloke, H. L.: Deriving global flood hazard maps of fluvial floods through a physical model cascade, Hydrol. Earth Syst. Sci., 16, 4143-4156, https://doi.org/10.5194/hess-16-4143-2012, 2012.

Revilla-Romero, B., Beck, H. E., Burek, P., Salamon, P., de Roo, A., and Thielen, J.: Filling the gaps: Calibrating a rainfall-runoff model using satellite-derived surface water extent, Remote Sens. Environ., 171, 118-131, https://doi.org/10.1016/j.rse.2015.10.022, 2015.

Ronchail, J., Cochonneau, G., Molinier, M., Guyot, J. L., Chaves, A. G. D. M., Guimarães, V., and De Oliveira, E.: Interannual rainfall variability in the Amazon basin and sea-surface temperatures in the equatorial Pacific and the tropical Atlantic Oceans, Int. J. Climatol., 22, 1663-1686, https://doi.org/10.1002/joc.815, 2002.

Sampson, C. C., Smith, A. M., Bates, P. D., Neal, J. C., Alfieri, L., and Freer, J. E.: A high-resolution global flood hazard model, Water Resour. Res., 51, 7358-7381, https://doi.org/10.1002/2015WR016954, 2015.

Schenk, C.J., Roland, J., Viger, R.J., Anderson, C.P.: Maps showing geology, oil and gas fields, and geologic provinces of the South America Region. U.S. Department of the Interior, USGS open-file report 97-470D, https://doi.org/10.3133/ofr97470D, 1999.

Schöngart, J., and Junk, W. J.: Forecasting the flood-pulse in Central Amazonia by ENSO-indices, J. Hydrol., 335, 124-132, https://doi.org/10.1016/j.jhydrol.2006.11.005, 2007.

Smith, P., Pappenberger, F., Wetterhall, F., Thielen, J., Krzeminski, B., Salamon, P., Muraro, D., Kalas, M., and Baugh, C.: On the operational implementation of the European Flood Awareness System (EFAS), ECMWF Tech. Memorandum, 778, 1–34, 2016.

Sood, A., and Smakhtin, V.: Global hydrological models: a review, Hydrol. Sci. J., 60, 549-565, https://doi.org/10.1080/02626667.2014.950580, 2015.

Sutanudjaja, E. H., Beek, R. V., Wanders, N., Wada, Y., Bosmans, J. H., Drost, van der Ent, R. J., de Graaf, I. E. M., Hoch, J. M., de Jong, K., Karssenberg, D., López López, P., Peßenteiner, S., Schmitz, O., Straatsma, M. W., Vannametee, E., Wisser, D., and Bierkens, M. F. P., N.: PCR-GLOBWB 2: a 5 arcmin global hydrological and water resources model, Geosci. Model Dev., 11, 2429-2453, https://doi.org/10.5194/gmd-11-2429-2018, 2018.

Timpe, K., and Kaplan, D.: The changing hydrology of a dammed Amazon, Sci. Adv. 3, e1700611, https://doi.org/10.1126/sciadv.1700611, 2017.

Thiemig, V., Rojas, R., Zambrano-Bigiarini, M., & De Roo, A.: Hydrological evaluation of satellite-based rainfall estimates over the Volta and Baro-Akobo Basin, J. Hydrol., 499, 324-338., https://doi.org/10.1016/j.jhydrol.2013.07.012, 2013.

Tomasella, J., Borma, L. S., Marengo, J. A., Rodriguez, D. A., Cuartas, L. A., A. Nobre, C., and Prado, M. C.: The droughts of 1996–1997 and 2004–2005 in Amazonia: hydrological response in the river main-stem, Hydrol. Processes, 25, 1228-1242, https://doi.org/10.1002/hyp.7889, 2010.

Trigg, M. A., Birch, C. E., Neal, J. C., Bates, P. D., Smith, A., Sampson, C. C., Yamazaki, D., Hirabayashi, Y., Pappenberger, F., Dutra, E., Ward, P. J., Winsemius, H. C., Salamon, P., Dottorri, F., Rudari, R., Kappes, M. S., Simpson, A. L., Hadzilacos, G., and Fewtrell, T. J.: The credibility challenge for global fluvial flood risk analysis, Environ. Res. Lett., 11, 094014, https://doi.org/10.1088/1748-9326/11/9/094014, 2016.

US Geological Survey.: Global 30 Arc-Second Elevation (GTOPO30), US Geological Survey, Center for Earth Resources Observation and Science (EROS), 1996.

van Beek, L. P. H. and Bierkens, M. F. P.: The Global Hydrological Model PCR-GLOBWB: Conceptualization, Parameterization and Verification, available at: http://vanbeek.geo.uu. nl/suppinfo/vanbeekbierkens2009.pdf (last access: 03 September 2018), 2008.

van Beek, L. P. H., Wada, Y., and Bierkens, M. F. P.: Global monthly water stress: 1. Water balance and water availability, Water Resour. Res., 47, W07517, https://doi.org/10.1029/2010WR009791, 2011.

van den Hurk, B. J. J. M., Viterbo, P., Beljaars, A. C. M., and Betts, A. K.: Offline validation of the ERA40 surface scheme, ECMWF TechMemo 295, Reading, UK, 2000.

van den Hurk, B. J., and Viterbo, P.: The Torne-Kalix PILPS 2 (e) experiment as a test bed for modifications to the ECMWF land surface scheme, Glob. Planet. Chang., 38, 165-173, https://doi.org/10.1016/S0921-8181(03)00027-4, 2003.

van Der Knijff, J. M., Younis, J., and De Roo, A. P. J.: LISFLOOD: a GIS-based distributed model for river basin scale water balance and flood simulation, Int. J. Geogr. Inf. Sci., 24, 189-212, https://doi.org/10.1080/13658810802549154, 2010.

van Huijgevoort, M. H. J., Van Lanen, H. A. J., Teuling, A. J., and Uijlenhoet, R.: Identification of changes in hydrological drought characteristics from a multi-GCM driven ensemble constrained by observed discharge, J. Hydrol., 512, 421-434., https://doi.org/10.1016/j.jhydrol.2014.02.060, 2014.

Wang, J., Hong, Y., Li, L., Gourley, J. J., Khan, S. I., Yilmaz, K. K., Adler, R.F., Policelli, F.S., Habib, S., Irwn, D., Limaye, A. S., Korme, T., and Okello, L.: The coupled routing and excess storage (CREST) distributed hydrological model, Hydrol. Sci. J., 56, 84-98, https://doi.org/10.1080/02626667.2010.543087, 2011.

Ward, P. J., Jongman, B., Salamon, P., Simpson, A., Bates, P., De Groeve, T., Muis, S., Coughlan de Perez, E., Rudari, R., Trigg, M. A., and Winsemius, H. C.: Usefulness and limitations of global flood risk models, Nat. Clim. Chang., 5, 712-715, https://doi.org/10.1038/nclimate2742, 2015.

Werner, M., Schellekens, J., Gijsbers, P., van Dijk, M., van den Akker, O., and Heynert, K.: The Delft-FEWS flow forecasting system, Environ. Model. Softw., 40, 65-77, https://doi.org/10.1016/j.envsoft.2012.07.010, 2013.

Wood, E. F., Roundy, J. K., Troy, T. J., Van Beek, L. P. H., Bierkens, M. F., Blyth, E., Roo, D.A., Döll, P., Ek, M., Famigiletti, J., Gochish, D., van de Giesen, N., Houser, P., Jaffé, P.R., Kollet, S., Lehner, B., Lettenmaier, D.P., Peters-Lidard, C., Sivapalan, M, Sheffield, J., Wade, A., and Whitehead, P.: Hyperresolution global land surface modeling: Meeting a grand challenge for monitoring Earth's terrestrial water, Water Resour. Res., 47, https://doi.org/10.1029/2010WR010090, 2011.

Xue, X., Hong, Y., Limaye, A., Gourley, J., Huffman, G., Khan, S., Dorji, C., and Chen, S.: Statistical and hydrological evaluation of TRMM-based Multi-Satellite Precipitation Analysis over the Wangchu Basin of Bhutan: Are the latest satellite precipitation products 3B42V7 ready for use in ungauged basins?, J. Hydrol., 499, 91–99, https://doi.org/10.1016/j.jhydrol.2013.06.042, 2013.

Yamazaki, D., Kanae, S., Kim, H., and Oki, T.: A physically based description of floodplain inundation dynamics in a global river routing model, Water Resour. Res., 47, https://doi.org/10.1029/2010WR009726, 2011.

Yamazaki, D., Lee, H., Alsdorf, D. E., Dutra, E., Kim, H., Kanae, S., and Oki, T.: Analysis of the water level dynamics simulated by a global river model: A case study in the Amazon River, Water Resour. Res., 48, https://doi.org/10.1029/2012WR011869, 2012.

Yamazaki, D., O'Loughlin, F., Trigg, M. A., Miller, Z. F., Pavelsky, T. M., and Bates, P. D.: Development of the global width database for large rivers, Water Resour. Res., 50, 3467-3480., https://doi.org/10.1002/2013WR014664, 2014a.

Yamazaki, D., Sato, T., Kanae, S., Hirabayashi, Y., and Bates, P. D.: Regional flood dynamics in a bifurcating mega delta simulated in a global river model, Geophys. Res. Lett., 41, 3127-3135, https://doi.org/10.1002/2014GL059744, 2014b.

Zajac, Z., Revilla-Romero, B., Salamon, P., Burek, P., Hirpa, F. A., & Beck, H.: The impact of lake and reservoir parameterization on global streamflow simulation, J. Hydrol., 548, 552-568., https://doi.org/10.1016/j.jhydrol.2017.03.022, 2017.

Zambrano-Bigiarini, M.: Package 'hydroGOF. Goodness-of-fit Functions for Comparison of Simulated and Observed Hydrological Time Series, http://www.rforge.net/hydroGOF/, last access: 25 September 2018, 2017.

Zhang, Y., Hong, Y., Wang, X., Gourley, J. J., Xue, X., Saharia, M., Ni, G., Wang, G., Huang, Y., Chen, S., and Tang, G.: Hydrometeorological analysis and remote sensing of extremes: Was the July 2012 Beijing flood event detectable and predictable by global satellite observing and global weather modeling systems? J. Hydrometeor., 16, 381-395, https://doi.org/10.1175/JHM-D-14-0048.1, 2015.

5   Zhang, Y., Zheng, H., Chiew, F. H., Arancibia, J. P., and Zhou, X.: Evaluating regional and global hydrological models against streamflow and evapotranspiration measurements, J. Hydrometeorol., 17, 995-1010, https://doi.org/10.1175/JHM-D-15-0107.1, 2016.

Zhao, F., Veldkamp, T. I., Frieler, K., Schewe, J., Ostberg, S., Willner, S., Schauberger, B., Gosling, S. N., Schmied, H. M., Portmann, F. T., Leng, G., Huang, M., Liu, X., Tang, Q., Hanasaki, N., Biemans, H., Gerten, D., Satoh, Y., Pkhrel, Y.,

10   Stacke, T., Ciais, P., Chang, J., Ducharne, A., Guimberteau, M., Wada, Y, Kim, H., and Yamazaki, D.: The critical role of the routing scheme in simulating peak river discharge in global hydrological models, Environ. Res. Lett., 12, 075003, https://doi.org/10.1088/1748-9326/aa7250, 2017.

Zsoter, E., Cloke, H., Stephens, E., de Rosnay, P., Muñoz-Sabater, J., Prudhomme, C., and Pappenberger, F.: How well do operational Numerical Weather Prediction setups represent hydrology?., J. Hydrometeorol., ~~in review,~~
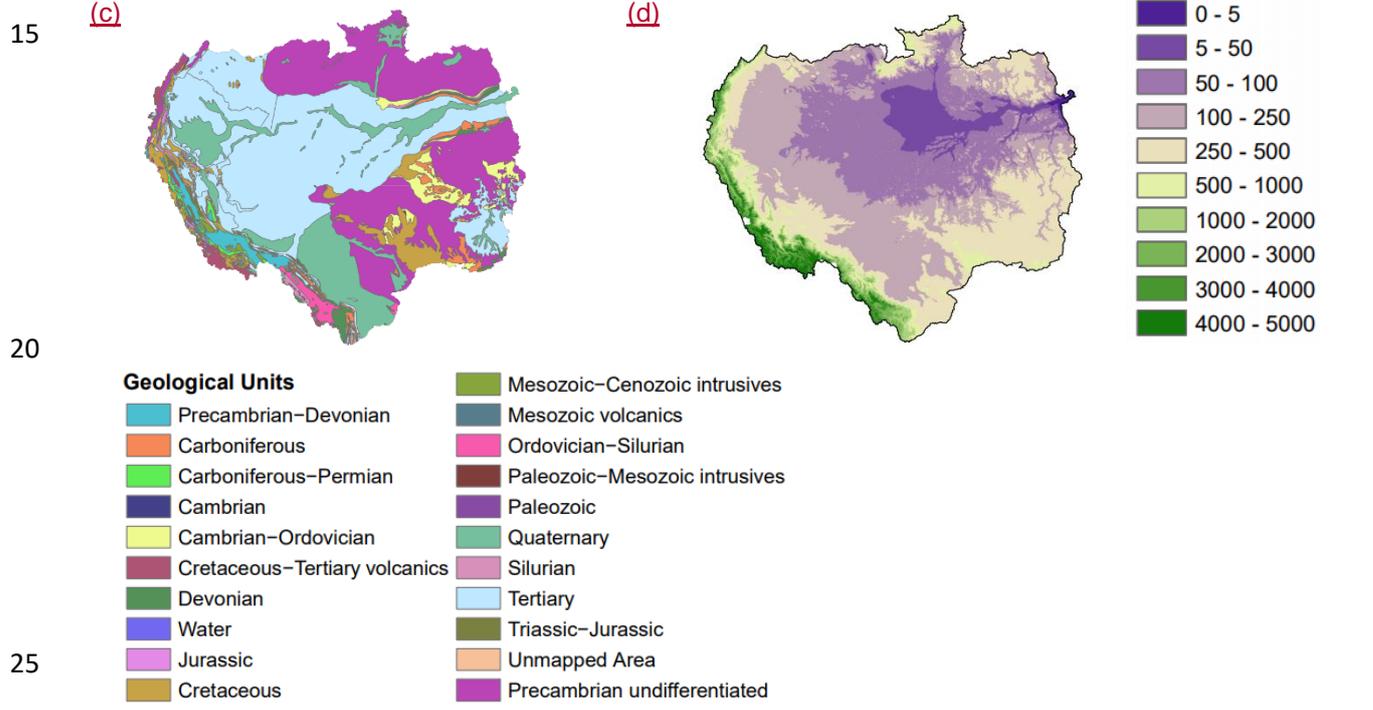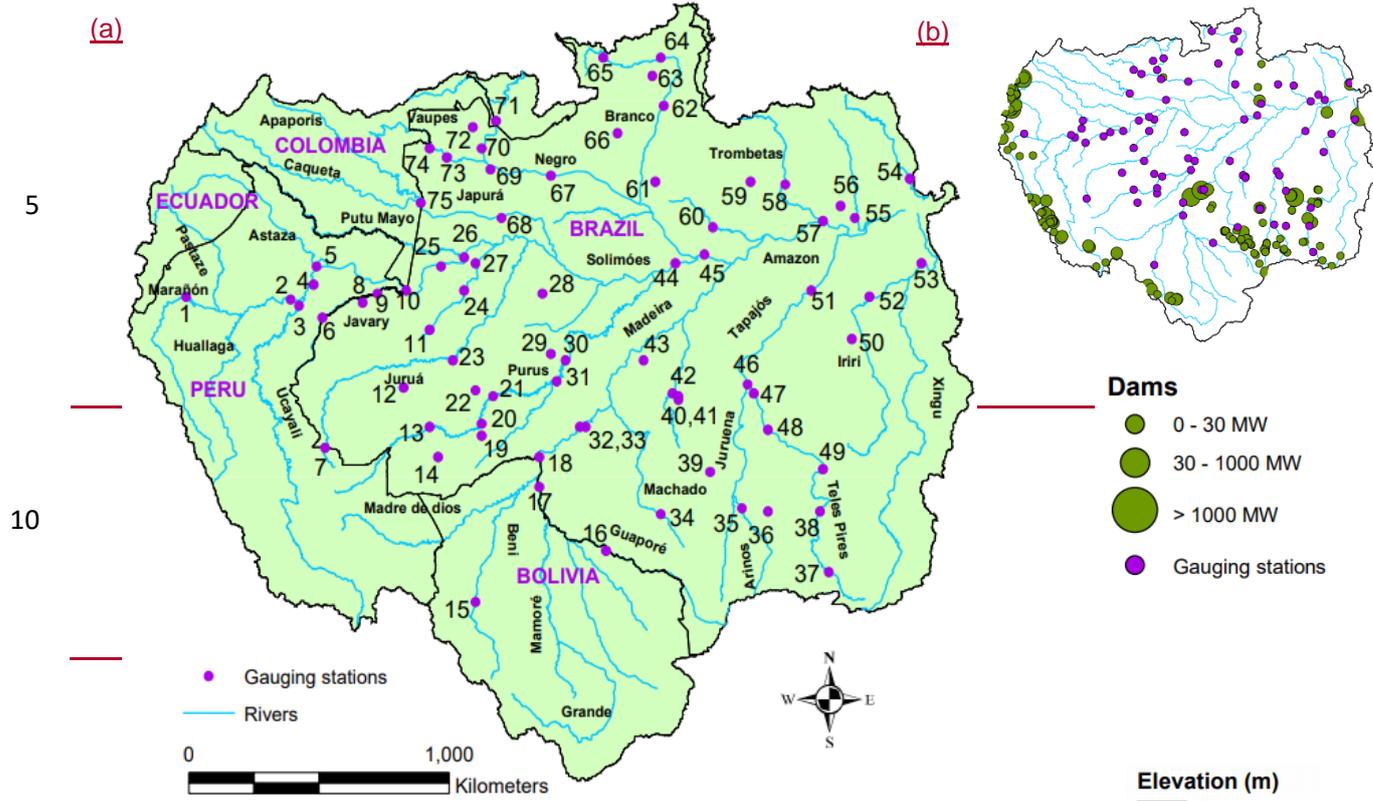
15   ~~2018.~~https://doi.org/10.1175/JHM-D-18-0086.1, 2019.

20

25

30

(a)

COLOMBIA
ECUADOR
PERÚ
BRAZIL
BOLIVIA

Apaporis
Vaupes
Caqueta
Astaza
Pastaza
Marañón
Huallaga
Putu Mayo
Javary
Juruá
Ucayali
Madre de dios
Beni
Mamoré
Grande
Negro
Branco
Trombetas
Japurá
Solimóes
Madeira
Purus
Machado
Guaporé
Amazon
Tapajos
Iriri
Juruena
Arinos
Teles Pires
Xingu

(b)

Dams
○ 0 - 30 MW
○ 30 - 1000 MW
○ > 1000 MW
● Gauging stations

● Gauging stations
— Rivers

0   1,000
Kilometers

N
W — E
S

(c)

(d)

Elevation (m)
■ 0 - 5
■ 5 - 50
■ 50 - 100
■ 100 - 250
■ 250 - 500
■ 500 - 1000
■ 1000 - 2000
■ 2000 - 3000
■ 3000 - 4000
■ 4000 - 5000

Geological Units
■ Precambrian–Devonian
■ Carboniferous
■ Carboniferous–Permian
■ Cambrian
■ Cambrian–Ordovician
■ Cretaceous–Tertiary volcanics
■ Devonian
■ Water
■ Jurassic
■ Cretaceous
■ Mesozoic–Cenozoic intrusives
■ Mesozoic volcanics
■ Ordovician–Silurian
■ Paleozoic–Mesozoic intrusives
■ Paleozoic
■ Quaternary
■ Silurian
■ Tertiary
■ Triassic–Jurassic
■ Unmapped Area
■ Precambrian undifferentiated

31

Figure 1: (a) Locations of the 75 hydrological gauges and the river network of the Amazon basin. Numbers represent stations which are referred to throughout the main text in italics. For station information see Table S1. (b) Locations of existing and under-construction dams as of 2017 (see Latrubesse et al., 2017). (c) Geological map of the Amazon (Schenk et al., 1999). (d) Elevation map of the basin from the digital elevation model (DEM) GTOPO30, at a horizontal resolution of approximately 1 km (USGS, 1996).

Table 1: Characteristics of the eight GHMs used to produce estimates of daily <u>river</u> discharge.

| Model Run	Meteorological forcing[1]	GHM[2]	GHM Spatial Resolution	Routing Model[3]	Routing Spatial Resolution	Temporal Resolution	Start	End	Calibration	Authors
ERA-I Land H-TESSEL Lisflood_uc	ERA-I Land	H-TESSEL	~0.75^0 (~80 km)	Lisflood	0.10^0 (~10 km)	Daily	01 Jan 1997	31 Dec 2015	None	Balsamo et al. (2015)[1] Balsamo et al. (2009)[2] van der Knijff et al. (2010)[3]
ERA-I Land H-TESSEL Lisflood_c	ERA-I Land	H-TESSEL	~0.75^0 (~80 km)	Lisflood	0.10^0 (~10 km)	Daily	01 Jan 1997	31 Dec 2015	See Hirpa et al. (2018)	Balsamo et al. (2015)[1] Balsamo et al. (2009)[2] van der Knijff et al. (2010)[3]
ERA-5 H-TESSEL Lisflood_uc	ERA-5	H-TESSEL	~0.28^0 (~31 km)	Lisflood	0.10^0 (~10 km)	Daily	01 Jan 1997	31 Dec 2015	None	See ECMWF (2018)[1] Balsamo et al. (2009)[2] van der Knijff et al. (2010)[3]
ERA-5 Lisflood H-TESSEL_c	ERA-5	H-TESSEL	~0.28^0 (~31 km)	Lisflood	0.10^0 (~10 km)	Daily	01 Jan 1997	31 Dec 2015	See Hirpa et al. (2018)	See ECMWF (2018)[1] Balsamo et al. (2009)[2] van der Knijff et al. (2010)[3]
Reforecasts H-TESSEL Lisflood_c	ECMWF 20-year control Reforecasts	H-TESSEL	~0.28^0 (~31 km)	Lisflood	0.10^0 (~10 km)	Daily	01 Jan 1997	31 Dec 2015	See Hirpa et al. (2018)	See ECMWF (2017)[1] Balsamo et al. (2009)[2] van der Knijff et al. (2010)[3]
ERA-I Land H-TESSEL CaMa-Flood	ERA-I Land	H-TESSEL	~0.75^0 (~80 km)	CaMa-Flood	0.25^0 (~25 km)	Daily	01 Jan 1997	31 Dec 2015	None	Balsamo et al. (2015)[1] Balsamo et al. (2009)[2] Yamazaki et al. (2011)[3]
ERA-I Land PCR-GLOBWB CaMa-Flood	ERA-I Land	PCR-GLOBWB	~0.50^0 (~50 km)	CaMa-Flood	0.25^0 (~25 km)	Daily	01 Jan 1997	31 Dec 2015	None	Balsamo et al. (2015)[1] Sutanudjaja et al. (2018)[2] Yamazaki et al. (2011)[3]
TRMM CRESTEF5	TMPA 3B42 v7. Real-time	EF5/CREST	~0.25^0 (~25 km)	EF5/CREST	0.05^0 (~5 km)	Daily	01 Jan 2003	31 Dec 2015	None	Huffman et al. (2007)[1] Wang et al. (2011)[2] Clark et al. (2016)[3]
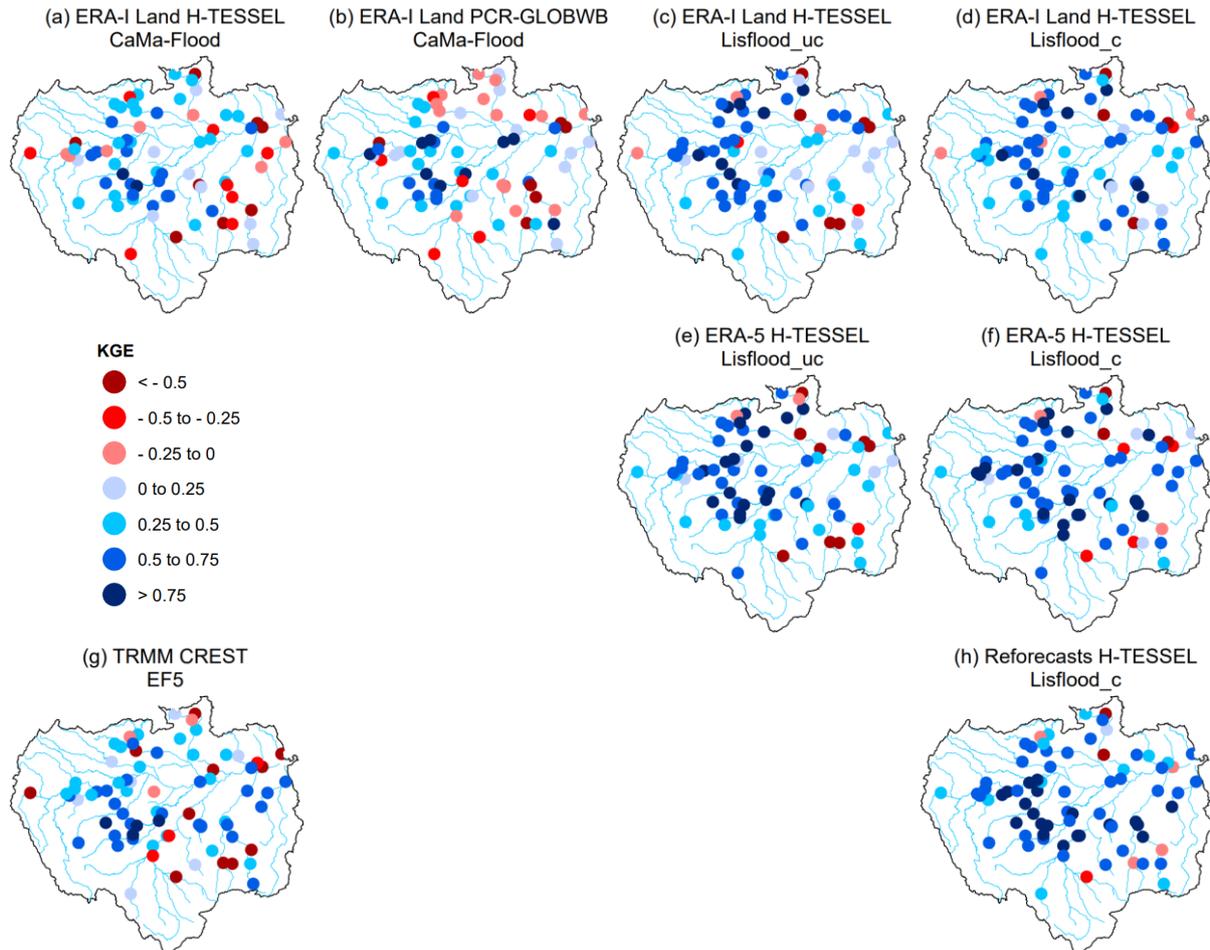
Figure 2: Full KGE scores at 75 hydrological gauging stations for all simulations ~~for~~. For the period 1997-2015 and 2004-2015 for CREST EF5 (g). Values greater than ~~zero~~0.75 are considered ~~skilful~~to indicate good performance (i.e. dark blue circles). To allow for easier model comparisons, plots are arranged by the different precipitation datasets (rows) and routing models (columns) with the exception of EF5 (g). For example, the final column consists of model runs using the calibrated Lisflood routing model.
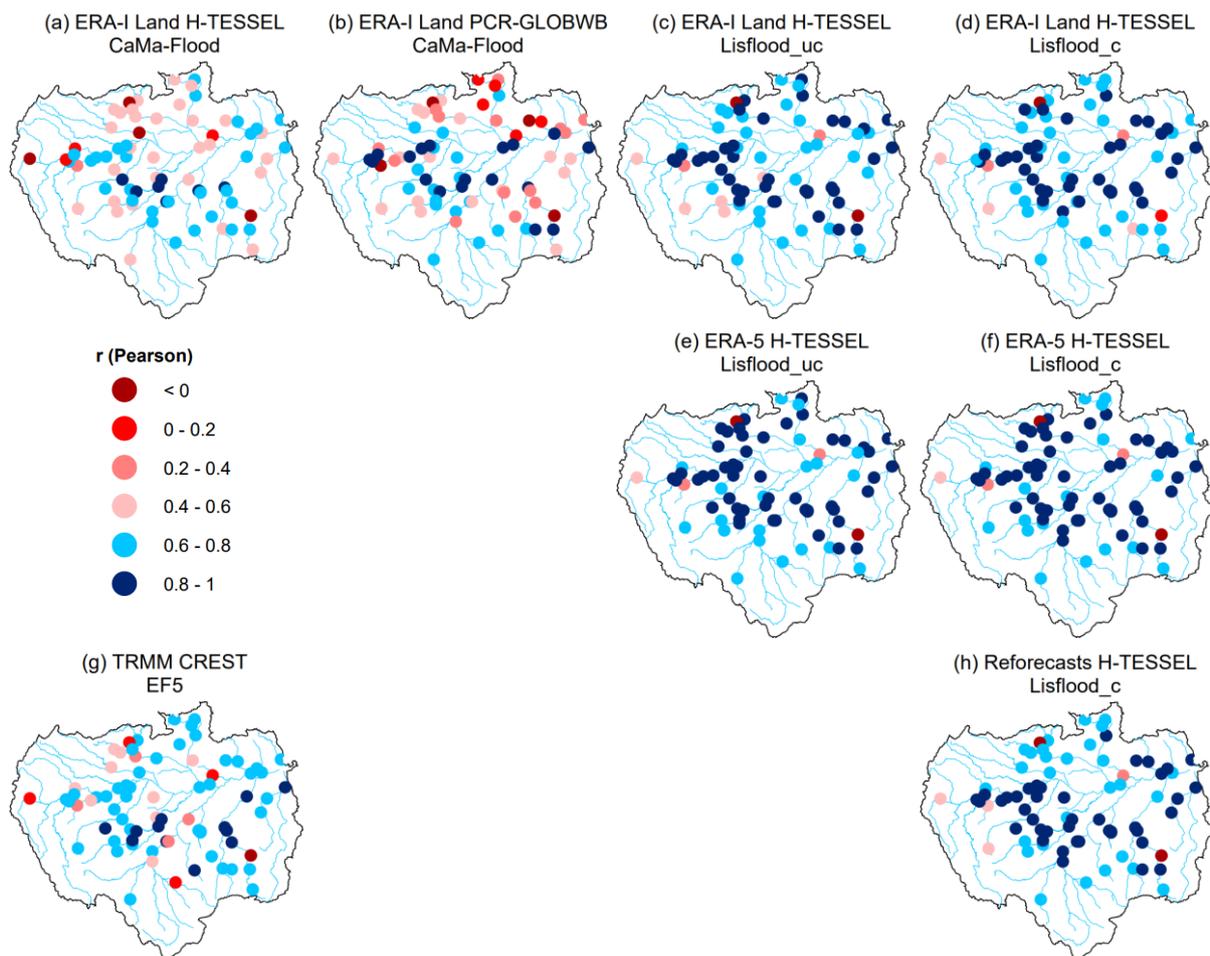
Figure 3: Correlation component of the KGE (Pearson's) at 75 hydrological gauging stations for all simulations ~~for~~. For the period 1997-2015 and 2004-2015 for CREST EF5 (g). Values greater than 0.6 are considered skilful (i.e. blue circles).
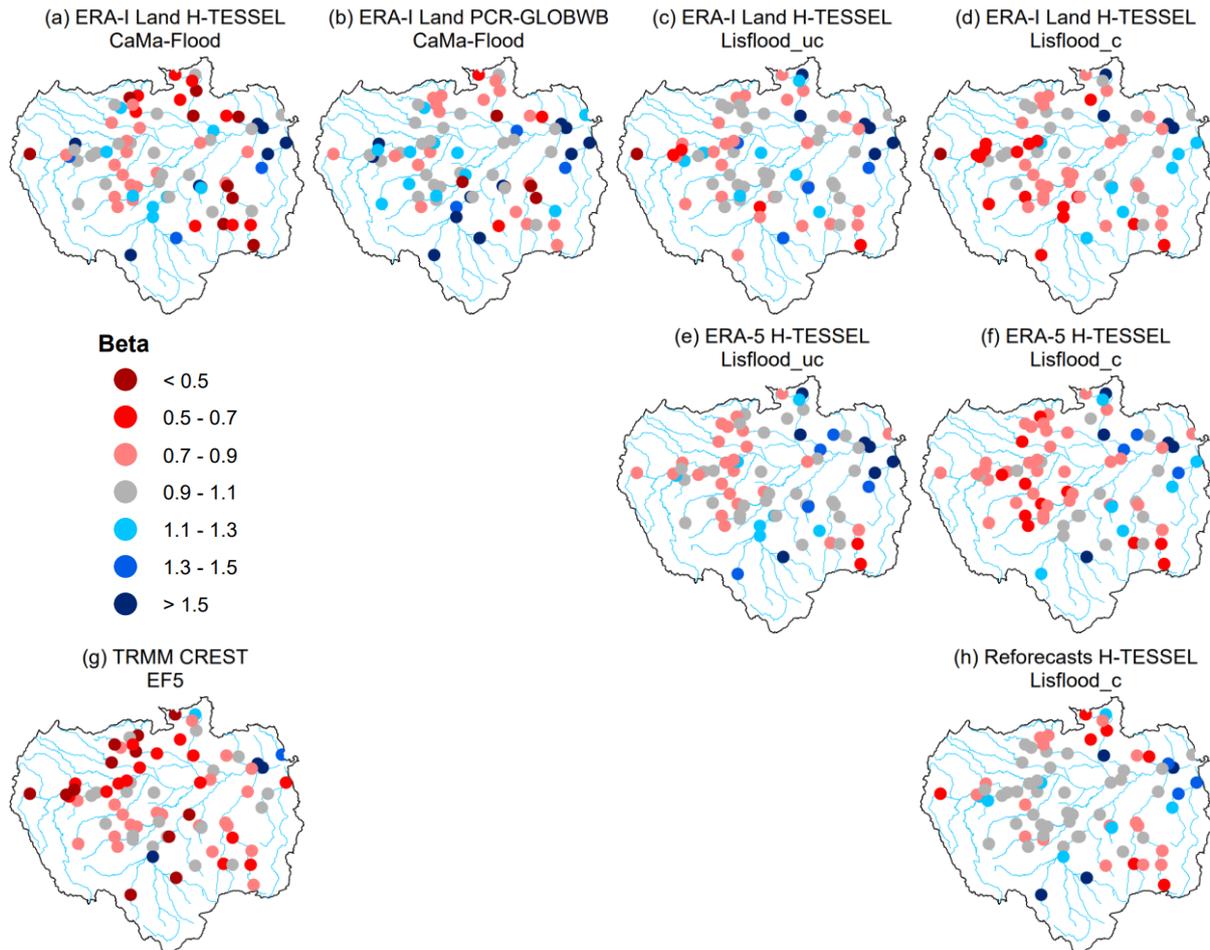
5

10
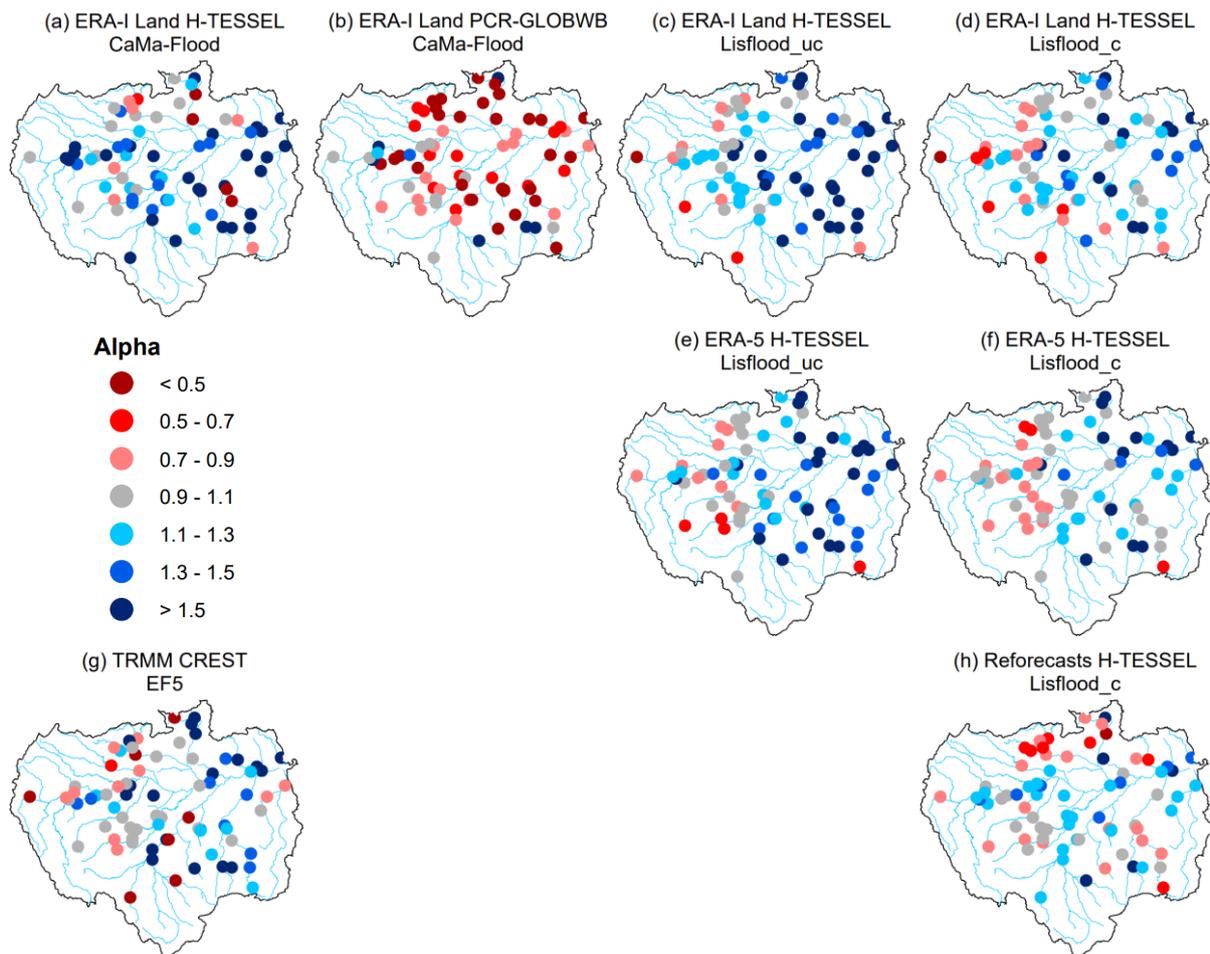
Figure 4: Alpha (i.e. variability ratio) component of the KGE at 75 hydrological gauging stations for all simulations for. For the period 1997-2015 and 2004-2015 for CREST EF5 (g). Blue circles indicate that the variability in the simulated time series is higher than that of the observed, while red circles show the opposite effect. Values closer to one indicate better model performance (i.e. grey circles).
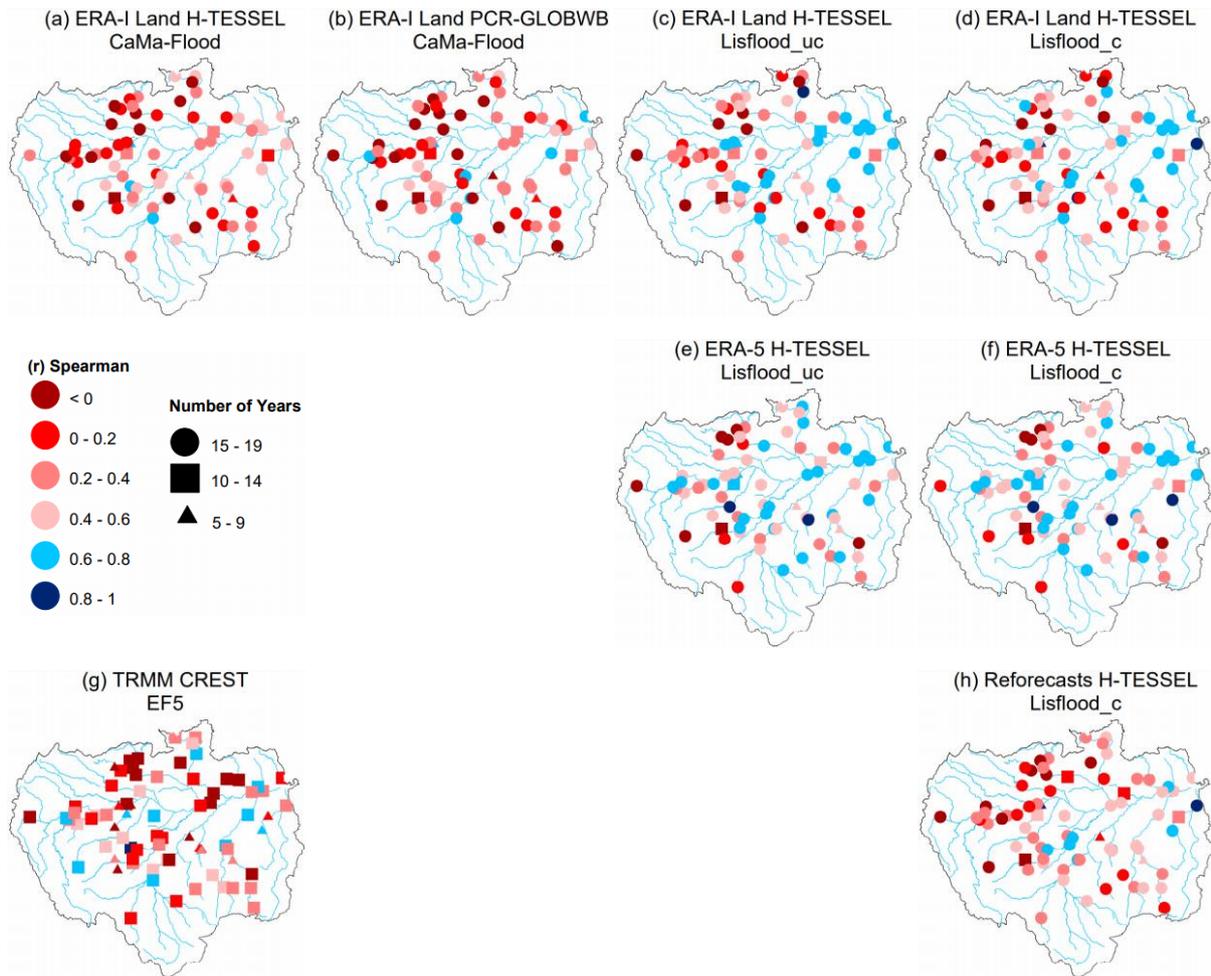
Figure 5: Beta (i.e. bias ratio) component of the KGE at 75 hydrological gauging stations for all simulations ~~for~~. For the period 1997-2015 and 2004 -2015 for CREST EF5 (g). Blue circles indicate that the bias in the simulated time series is higher than that of the observed, while red circles show the opposite effect. Values closer to one indicate better model performance (i.e. grey circles).

5

Figure 6: Spearman's ranked correlation coefficients for observed against simulated annual maximum discharge at 75 hydrological gauging stations for all simulations ~~for~~. For the period 1997-2015 and 2004-2015 for CREST EF5 (g). Values exceeding 0.6 are considered skilful (i.e. blue shapes). Number of overlapping years of data between observations and simulations are denoted by different shapes ~~(e.g.~~. A triangle represents 5-9 years, a square 10-14 years and a circle ~~for~~ 15-19 years of overlapping data~~).~~.
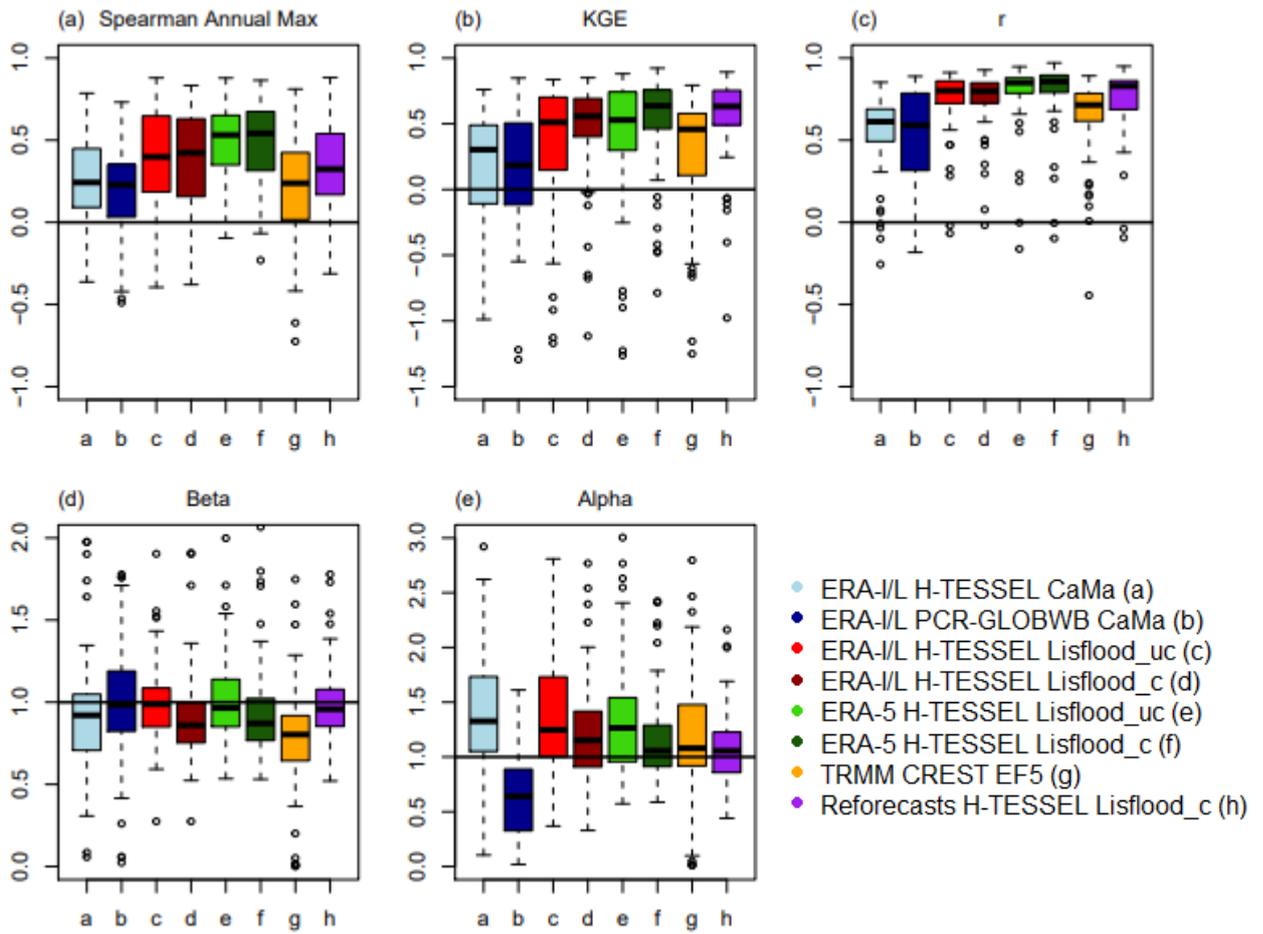
Figure 7: Boxplots showing the distribution of scores for the (a) Spearman correlation coefficient (annual maximum), (b) KGE, (c) KGE Pearson's rho, (d) KGE beta and (e) KGE alpha, for all simulations.

5

10

Table 2: ~~Mean~~Median **scores for the 75 hydrological gauging stations for all metrics.**

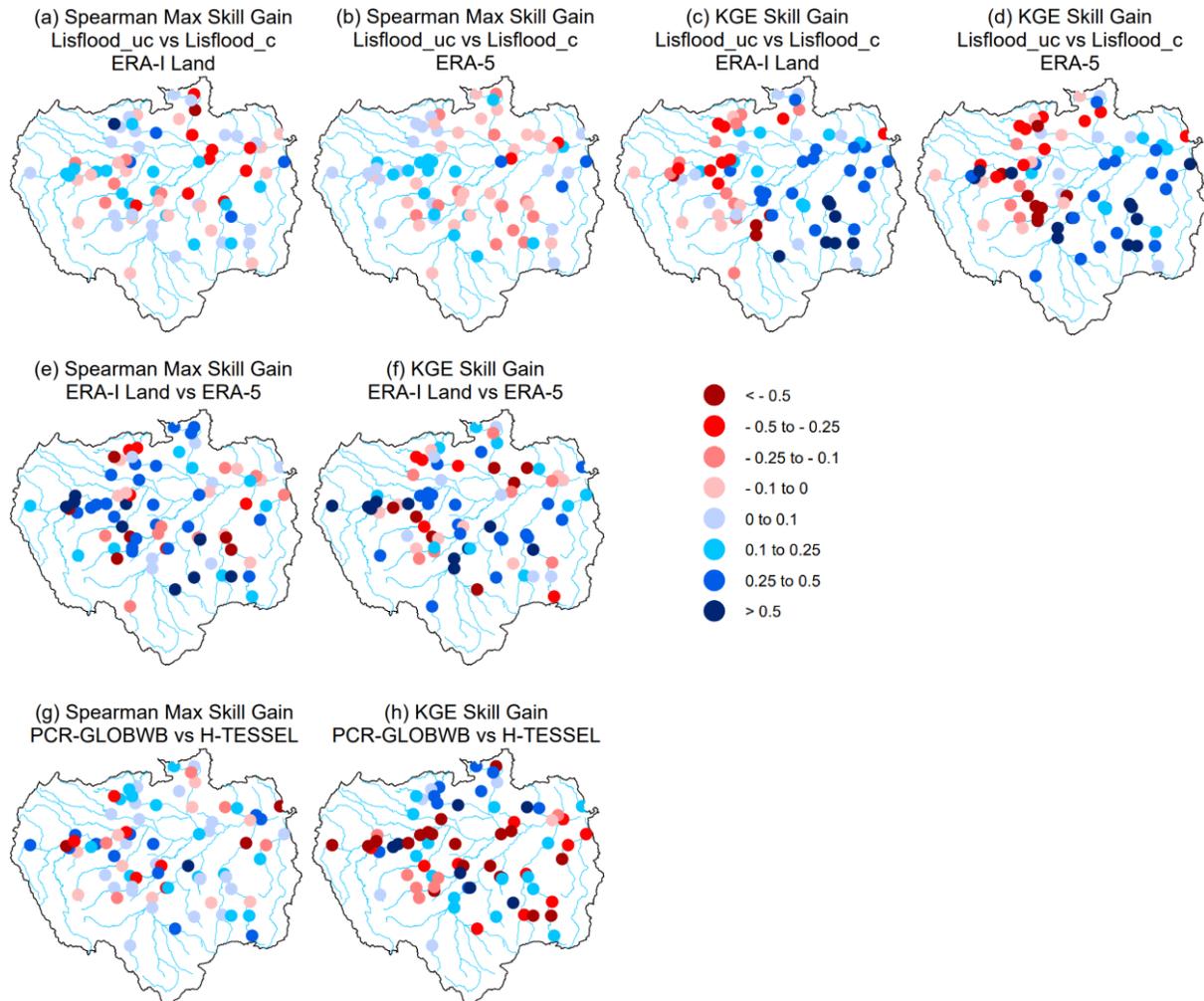| Model Runs	Spearman Annual Max Correlations	KGE	r (Pearson's)	Beta	Alpha
ERA-Interim Land H-TESSEL CaMa-Flood	0.~~25~~24	0.~~03~~30	0.~~57~~61	0.~~98~~92	1.~~53~~33
ERA-Interim Land PCR-GLOBWB CaMa-Flood	0.~~19~~23	0.~~10~~18	0.~~53~~59	~~1.12~~0.98	0.~~74~~64
ERA-Interim Land H-TESSEL Lisflood_uc	0.~~37~~40	0.~~23~~51	0.~~75~~80	~~1.04~~0.99	1.~~51~~25
ERA-Interim Land H-TESSEL Lisflood_c	0.~~37~~42	0.~~37~~56	0.~~75~~80	0.~~92~~86	1.~~31~~15
ERA-5 H-TESSEL Lisflood_uc	0.~~48~~53	0.~~27~~63	0.~~79~~85	~~1.09~~0.97	1.~~47~~26
ERA-5 H-TESSEL Lisflood_c	0.~~48~~54	0.~~41~~64	0.~~80~~86	0.~~97~~87	1.~~28~~06
TRMM CREST EF5	0.~~21~~24	0.~~16~~46	0.~~65~~71	0.~~78~~80	1.~~32~~08
Reforecasts H-TESSEL Lisflood_c	0.~~33~~32	0.~~53~~63	0.~~76~~83	~~1.00~~0.96	1.~~10~~06
~~Mean~~Median across models	0.~~34~~35	0.~~26~~50	0.~~70~~78	0.~~99~~91	1.~~28~~11

5

10
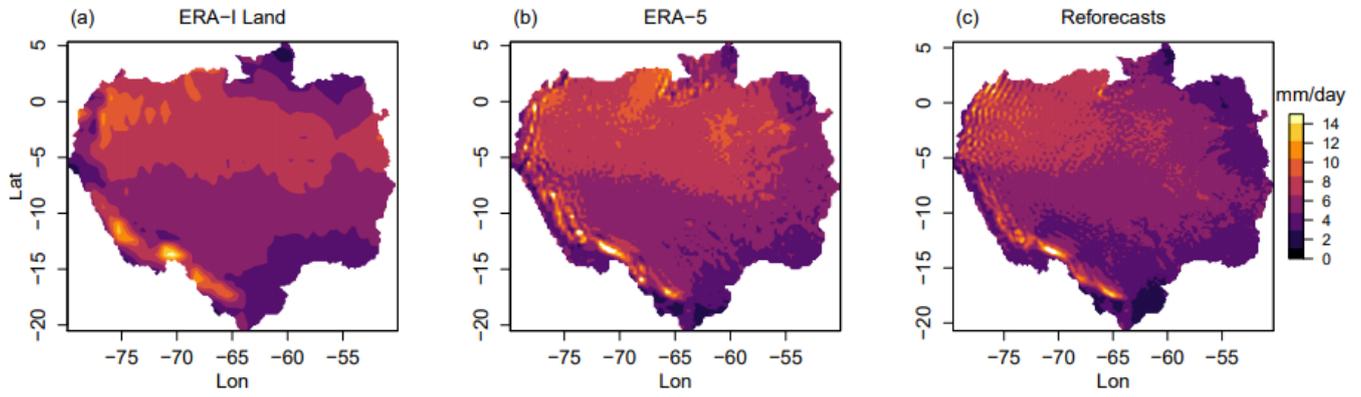
Figure 8: Mean daily precipitation throughout the Amazon basin, for (a) ERA-Interim Land, (b) ERA-5 and (c) the ECMWF 20-year reforecasts. For the period 1997-2015.

5

10

15

Figure 8Figure 9: Relative improvement in skill at each gauging station for Spearman annual maximum correlations and KGE values (i.e. skill scores). (a-d) show relative gain or loss in skill when using the newly calibrated Lisflood run (Lisflood_c) relative to the uncalibrated model run (Lisflood_uc)), using precipitation forcing from both the ERA-Interim Land and ERA-5 reanalysis products. (e-f) showshows the relative gain or loss in skill when using ERA-5 as opposed to ERA-Interim Land. (g-h) showshows the relative gain or loss in skill when using the LSM H-TESSEL rather thancompared to the hydrological model PCR-GLOBWB. All scores are calculated using the skill scores in Eq. (1). Red indicatescircles indicate a decrease in skill, whereas blue representscircles represent an increase.
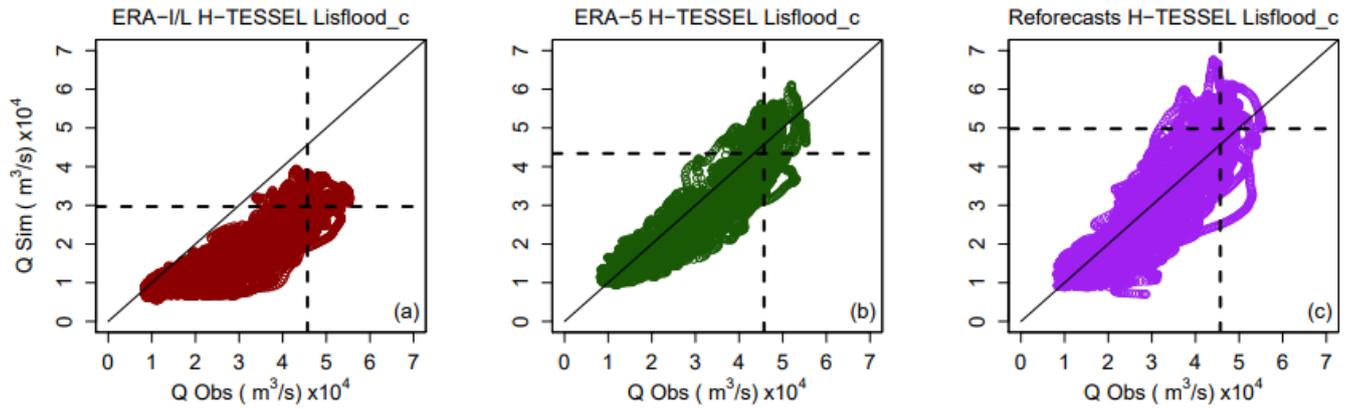
10

Figure 910: Scatterplots of observed against simulated river flow at the Tamshiyacu gauging site, Peru (*4*). For (a) ERA-Interim Land, (b) ERA-5 and (c) the ECMWF 20-year reforecasts forced through the calibrated Lisflood routing model. Dashed black lines indicate the observed and simulated 90th percentile of river flow. For the period 1997-2015.

5